Die approbierte Originalversion dieser Diplom-/Masterarbeit ist an der Hauptbibliothek der Technischen Universität Wien aufgestellt (http://www.ub.tuwien.ac.at).

The approved original version of this diploma or master thesis is available at the main library of the Vienna University of Technology (http://www.ub.tuwien.ac.at/englweb/).

Diplomarbeit

Master's Thesis

Feasibility study of a hydraulically operated marine current power plant

carried out for the purpose of obtaining the academic degree of Graduate Engineer under the guidance of

Senior Lecturer Dr. Andrew Grant
Mechanical Engineering Department
University of Strathclyde, Glasgow, UK
and
Em.O.Univ.Prof. Dipl.-Ing. Dr.techn. Dr.h.c. Heinz-Bernd Matthias
E302 - Institute for Thermodynamics and Energy Conversion
TU Vienna

handed in at the Technical University of Vienna
Faculty of Mechanical Engineering and Science of Management

by

Sascha Polak
Reg. No.: e9825691
Elisabethstr. 17
3001 Mauerbach

Glasgow, 17. August 2007

Acknowledgments

First and most important I want to express my gratitude to my wife Christiane, who has become the most important person in my life in the last two years and always supported me during my thesis in Scotland.

Furthermore, I want to give thanks to my valuable parents, Silvia and Peter, for their extensive backup throughout my years of study, not forgetting my two sisters, Barbara and Katharina, and my brother Manuel.

Finally, I thank my supervisors of Strathclyde University, Dr. Andrew Grant and Dr. Gray Connor, who have been a pleasure to collaborate with.

Abstract

As the Scottish government is becoming more interested in shifting their energy production from oil and nuclear power to renewable and cleaner methods, the University of Strathclyde is involved in a project to examine the possibilities of generating electricity from tidal streams, which especially occur on Western Scottish shores due to their cleft landscapes.

These fjords and canals work like tube constrictions and accelerate the tidal flow significantly. In contrast to barrage tidal power plants which utilise the potential energy from the difference in height, power production is sought by positioning turbines into the water current.

Concretely, the tidal turbine consists of two counter-rotating rotors sitting on one axle, which means that the overall turbine system produces effectively zero torque. Although there is certainty about the actual turbine design, the transmission technique between turbine and generator is still uncertain and needs further investigations.

My thesis is about the feasibility of installing a hydraulic drive train into a marine current turbine. As this method is at first glance more complex than a mechanical connection, it also provides some freedom in configuring the plant system, because of the separation of both devices.

Specifically, I investigated the dimensions and specifications of all required units of a 300 kW - power plant and gave an overview on configuration, set-up, maintenance and installation issues. Moreover, I tested the drag force of a small-scale turbine model in a test tank.

Table of contents

1. Introduction 1
1.1. Background 1
1.2. General power plant design 3
1.3. Power transmission 4

2. Turbine Design 9
2.1. Turbine theory 9
2.2. Turbine specifications 11

3. Drive train design and specifications 14
3.1. Pumps 14
3.1.1. Selecting pump model 14
3.1.2. Further pump specifications 17
3.1.2.1. Charge Pressure P_C (valid for a case pressure of 1 bar) 17
3.1.2.2. Pressure loss Δp_L 17
3.1.2.3. Flow rate q 18
3.1.3. Hydraulic oil requirements 19
3.1.4. Pump efficiency 20
3.2. Hydraulic motor – generator combination options 21
3.3. Hydraulic motor specifications 23
3.3.1. Further hydraulic motor specifications 25
3.3.2. Flushing 26
3.3.3. Oil selection 26
3.3.4. Service intervals 28
3.3.5. Controlling 28
3.4. Generator specifications 29
3.5. Hoses 30
3.5.1. Dimension requirements 30
3.5.2. Selecting hose model 31
3.5.2.1. Defining turbulence in hose 32
3.5.2.2. Expenses 33
3.5.2.3. Other issues 33

4. Power plant design 34
4.1. Turbine 34
4.1.1. Buoyancy 34
4.1.2. Turbine base construction: method 1 34
4.1.2.1. Drag force of turbine 35
4.1.2.2. Horizontal angle of turbine 36
4.1.2.3. Air tank volume 38
4.1.3. Turbine base construction: method 2 39
4.1.3.1. Overall concept 39
4.1.3.2. Air tank volume 40
4.1.3.3. Base dimensioning 40
4.1.3.4. Dimensioning of main pole 41
4.1.3.5. Dimensioning of supporting poles 42
4.1.3.6. Rope dimensions 43
4.1.3.7. Considerable points 44
4.2. Generator Base - Platform 46
4.2.1. Platform size 46
4.2.2. Drag force on platform 47
4.2.3. Specifications of generator base 48
4.2.4. Platform – Base connection 49
4.2.4.1. Force on rope 50

5. Testing: Turbine drag force 51
5.1. Betz Theory 52
5.2. Mesh test in duct 53
5.2.1. Calculating drag force of mesh 53
5.2.2. Test of meshes in duct 55
5.2.2.1. Without mesh 56
5.2.2.2. With mesh 59
5.2.2.2.1. Mesh A - Square mesh with round threads 60
5.2.2.2.2. Mesh B - flat mesh with round holes 61
5.2.2.2.3. Mesh C - square flat mesh 62
5.2.3. Results 63
5.3. Test series in water tank 64
5.3.1. Pre-test procedure 64

5.3.2. Test runs 65
5.3.2.1. Testing drag force of mesh A – day 2 67
5.3.2.2. Testing drag force of mesh C – day 2 67
5.3.3. First conclusions 67
5.3.4. Comparing test results with calculations 68
5.3.5. Further considerable aspects 71

6. Implementation issues 72
6.1. Maintenance 72
6.1.1. Solution method 1 72
6.1.2. Solution method 2 74
6.1.2.1. General 74
6.1.2.2. Lifting bags 76
6.1.2.3. Rope size 78
6.1.2.4. Air bag size 79
6.1.2.5. Disadvantages of method 2 80
6.1.3. Other approaches 81
6.2. Set up 82

7. Configuration perspectives 84

8. Conclusion 86

A Graphical excerpt 88

B Bibliography 94

C List of variables 96

1. Introduction

1.1. Background

In these days where *global warming* and *climate change* are lively discussed issues by all concerned people around the globe, it becomes more and more important to think of alternative strategies than using fossil fuels to produce energy. Nature provides us with lots of different kinds of energy resources - like water-, wind- or sun energy – which are nearly ubiquitous available around the world.

One possibility to reduce CO_2 emissions is to produce electric energy from the tidal power of the water. The moon is the major contributor of the tidal flow. The fact that the earth turns around its own axis in 24 hours and the moon needs for one circulation around the earth 4 weeks leads to a period of 12 hours and 24 minutes for a tidal cycle. The power of the tide can change however due to gravitational interactions between the sun and the moon. If these two objects enforce their gravitational impact on the oceans, we call it *spring tide*. If they abate each other, it is called *neap tide*. There are also some other smaller variations of the tidal power caused by the elliptical orbits of the moon and the earth. Beside the described fluctuations the tidal flow speed is a steady sinusoidal curve.

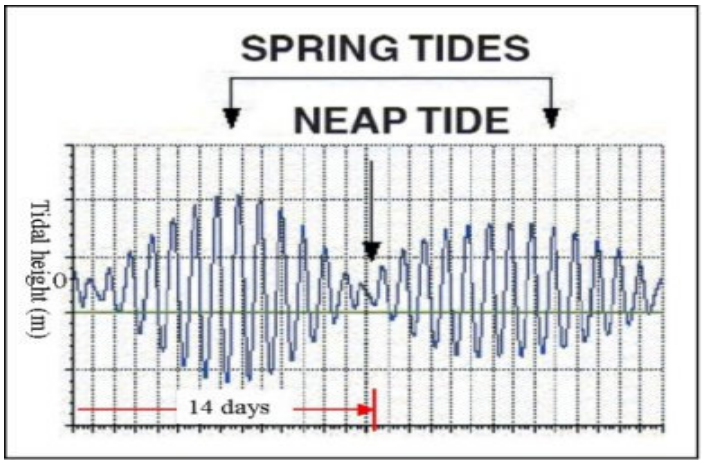

Picture 1.1

This leads to a unique characteristic of the tides, which makes them outstanding compared to other natural energy resources. *Their movements are fully predictable*. This fact makes a possible utilisation of tidal energy a far easier task. One major problem for example with wind turbines is that they might not produce electricity in times of high demand, whereas

the power producing timeslots of tidal turbines are well-known and therefore can be taken into consideration for a proper electricity supply plan.

However, the usual tidal ranges around the coastlines on the world are far too low to be capable of producing electricity. It needs geographic ally outstanding sites, like fjords or channels, flanked by an ocean, which are able to concentrate the tidal force in order to increase the tidal range and consequently the flow velocity. Seas like the Mediterranean Sea are too small to cause enough inertia.

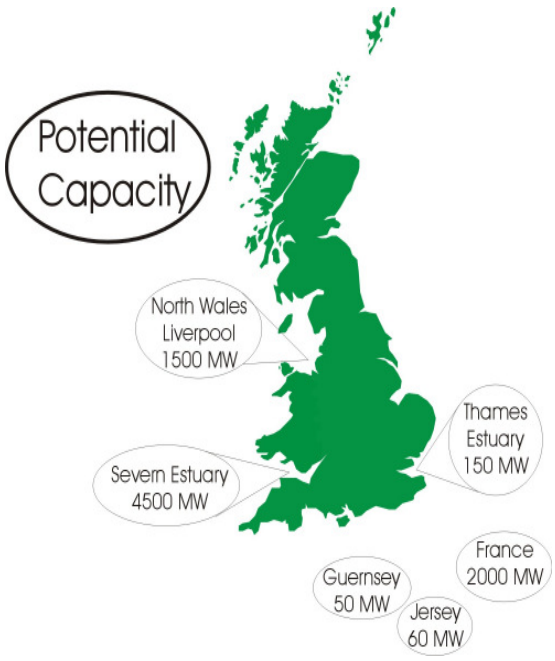

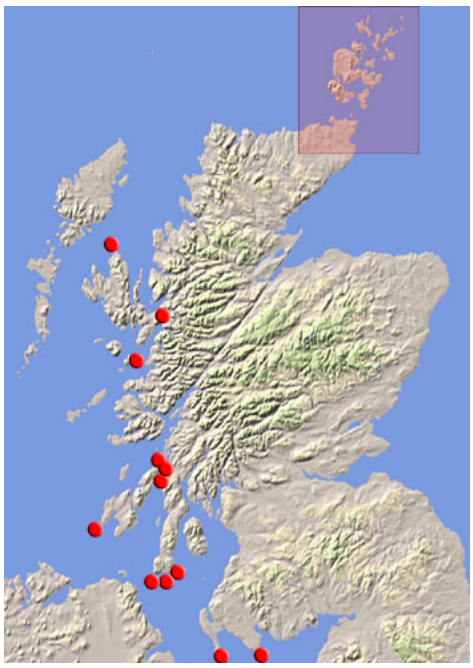

Pictures 1.2 & 1.3

Animation of world wide tidal flow: http://upload.wikimedia.org/wikipedia/commons/b/b2/Animation_fes2004.gif

One possibility to generate electricity from the tide is building a barrage and creating a tidal lagoon. However, suitable places are rare and environmental impact is estimated to be devastating as large marine areas need to be enclosed.

Another common method is producing electric energy from the tidal stream via water turbines. This solution is estimated to be a more promising, because firstly turbines are able to generate electricity in both flow directions and secondly can be built in various dimensions depending on demand and area. Furthermore, the amount of capital invested is much smaller, turbine farms can be extended if required, technical approval is easier and the environmental impact is considered to be far lower compared to tidal barrage systems.

A site gets economically interesting, when the maximum flow velocity gets well above the 2 m/s - mark. A water depth of around 30 m is considered to be optimal.

1.2. General power plant design

Designing a marine current turbine is quite similar to designing a wind turbine as the same theoretical background applies for both. According to 'Betz' law' (*reference 1*) a wind turbine produces maximum power, when the wind speed behind the rotor is 1/3 of the original wind speed. This means that the turbine can utilize maximal 59.3% of the available wind energy. So the *power coefficient* c_P has a maximum value: $c_{p,max} = 0.593$. In practice the values of c_P lie between 0.4 and 0.5 for modern rotors.

However, levels of turbulence and velocity in water are different to them in air, because tidal streams are normally bi-directional whereas wind tends to be multi-directional. Furthermore, tidal currents have well-known territory-depending velocity limits compared to relatively random wind currents.

The main difference in this project, when compared to other prototypes, is that this turbine consists of two counter-rotating rotors placed in a close back-to-back formation attached to the same shaft. The upstream rotor possesses 3 whereas the downstream rotor accommodates 4 blades. This is due to a slightly higher rotational speed of the upstream rotor.

This layout has the following advantages:

- near-zero reaction torque on the supporting structure
- near-zero swirl in the wake of the turbine
- Increased relative shaft output speed
- Increased space efficiency

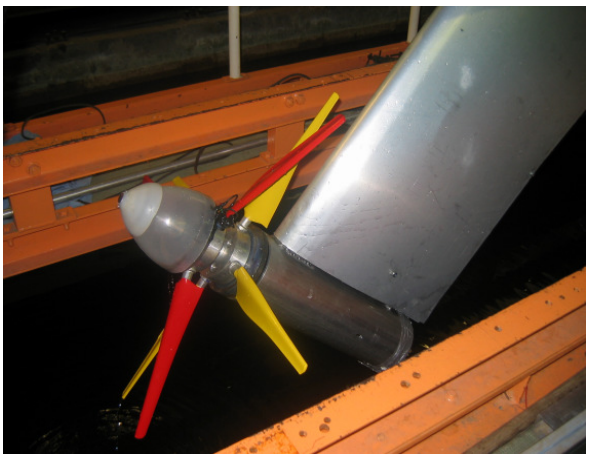
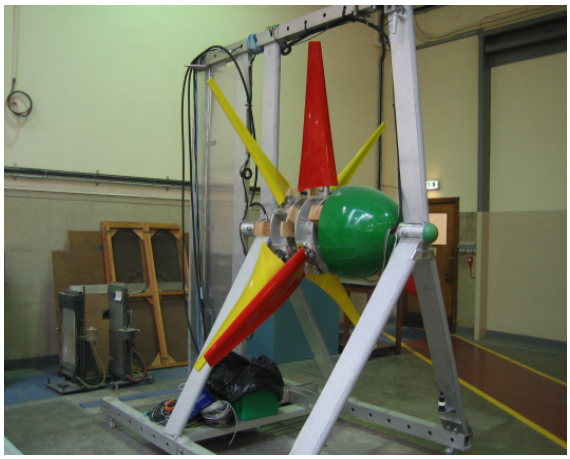

Pictures 1.4 & 1.5

To get an impression of this ongoing project, the left picture above shows the first prototype with a diameter of 0.8 meters attached to a carriage in a test tank. The upstream rotor is marked red and the downstream rotor is yellow. The power connection is accomplished by two axles which hidden behind the wing-shape casing. The right picture shows a scale-up of the preceding model with 3 meters in width.

1.3. Power transmission

This project is based on the idea of a counter-rotating turbine design, which is one of the unalterable facts of this thesis. My work is to find an appropriate solution of transmitting the power from the turbine to the generator.

The fact that we have a counter- rotating turbine, which produces no torque on the overall, provides us some freedom in the way of arraying the specified devices. The idea is to take advantage of the zero net reaction torque and to let the turbine float in the water. Therefore, we have to ensure that the overall density of the turbine is lower than water (seawater density ~ 1025 g/cm³) in order to realise stable floatation. For fixation we use a high-duty cable wire to link the turbine and the seabed.

The tidal stream's velocity over time has the shape of a sinusoidal curve (diagram 2.2, page 10) or in other words the velocity and the direction of the tide changes over time. For this reason there need to be an adjustment, specifically the turbine has to turn 180° after each half tide period in order to be placed towards the current. So by designing a free moving turbine the overall construction can become simpler.

The advantage of this constellation is the self-aligning ability of the turbine depending on the current direction. The turbine always points exactly at the flow direction. The attachment can be compared to a pendulum which is mounted upside-down (Sketch 1.1). Consequently, there is no need for an external adjustment of the turbine's direction which leads to cost reduction.

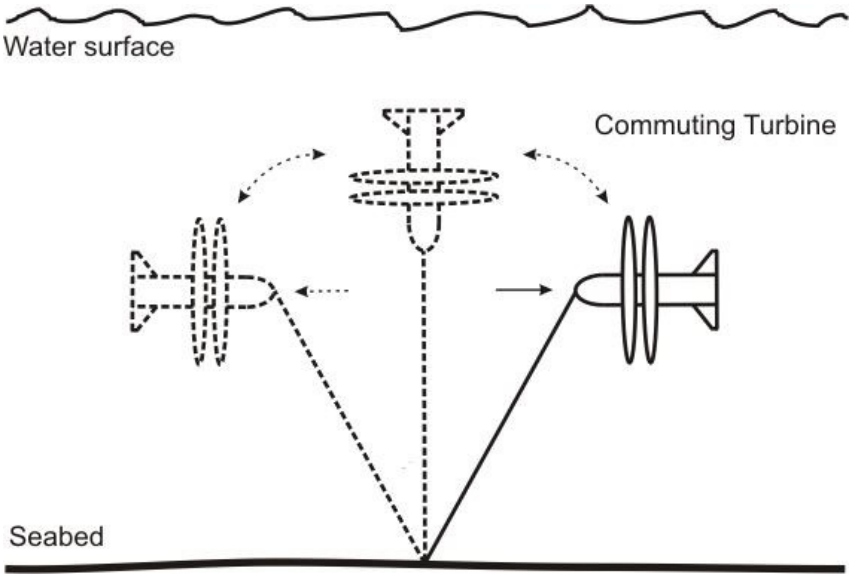

Sketch 1.1

A lot of other marine current turbine projects build massive concrete bases (pictures 1.6 - 1.8 on page 6) and fix the turbine on those. The disadvantages of these systems are for example higher construction costs, but also increasing difficulty to uninstall the system after a lifetime cycle. It is also necessary to assemble a lift on the turbine station to heave the turbine for inspection or maintenance. The idea in this project is to omit expensive massive structures like shown below and consequently to reduce the costs significantly.

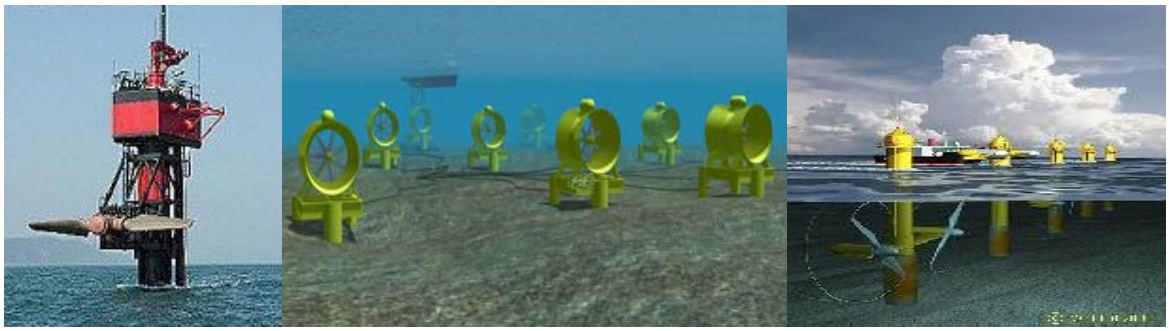

Pictures 1.6, 1.7 & 1.8

A free floating power plant would mean that the generator has to be placed into the turbine casing to achieve a mechanical connection to the turbine. However, another initial condition of this survey is to place the generator on the water surface for better accessibility and not utilise a wet running generator.
Generators in sub-sea conditions are quite problematic to operate, because cooling with seawater is unlike due to salinity (300 kW-machines can also work without cooling). Secondly, generators need to be adapted to under-sea-conditions, which is expensive. So to keep costs and reliability low, the generator is located above sea level.

As there is no other realistic solution for a mechanical connection, a hydraulic power transmission looks feasible. Still, on account of our system we need two pumps, each one linked over an axle to one of the turbines, which run in opposite directions. Here occurs the first problem. The easiest solution would be a pump-turbine-pump-turbine constellation in the casing. This is not realisable, because the hoses of the pumps have to be led out on the front end of the casing. Therefore the hose pair of the downstream turbine would have to pass the upstream turbine, which is impossible.

The solution is to place both pumps in front of the two turbines, having a pump (upstream) - pump (downstream) - turbine (upstream) - turbine (downstream) constellation. This configuration leads to the necessity of a shaft rotating in a counter-rotating hollow shaft. The downstream turbine transmits the power over a solid shaft to the downstream pump respectively the upstream turbine transmits the power over the hollow shaft to the upstream pump. The mechanical advantage of this design is to have a short hollow shaft and a long solid shaft as the hollow shaft needs not be dimensioned excessively.

The next element in the system is the attachment of the rope wire coming from the turbine to the bottom of the sea. We could mount the wire directly to the seabed, for example by drilling a massive metal anchorage in the ground combined with a clamp to hold the wire. Thus we would need a team of divers for mounting/demounting the system not mentioning repair issues.
Another chance is to attach the steel wire to a massive concrete block, which is just placed on the seabed without actually anchoring it to the ground. That would give us the freedom to heave and sink the device whenever it is required, e.g. for consecutive inspections and

services. It would also ease uninstalling the plant after a full life cycle and lower the environmental aftermath.

However, the consequence of omitting an anchorage point is that the concrete base needs to be dimensioned massively, that it is able to withstand the rated drag force and buoyant force caused by the turbine. That means that the weight of the base has to be significantly higher than the rated drag force.

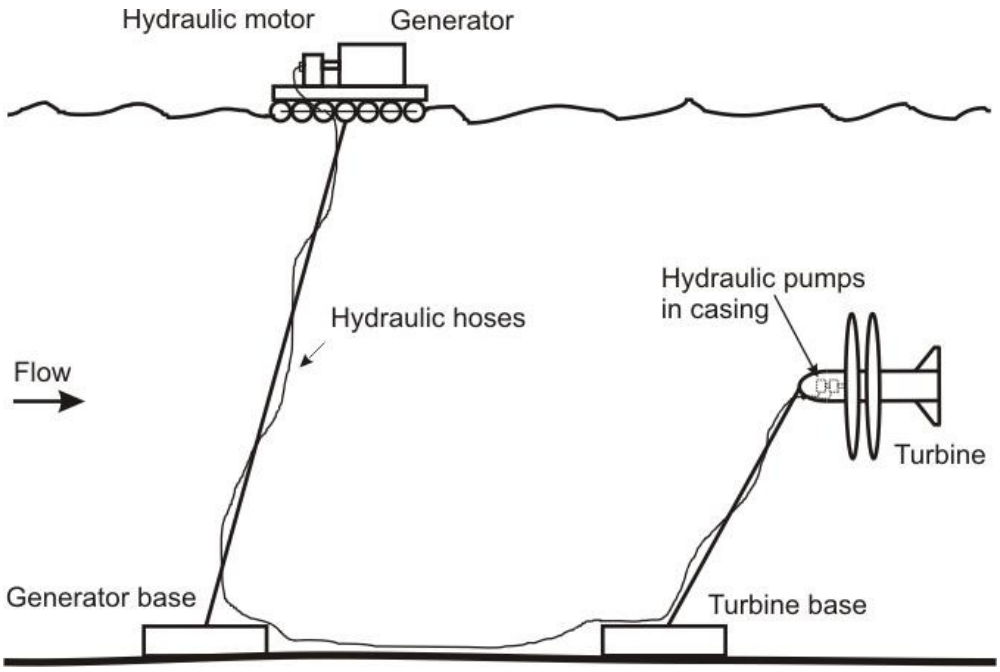

Sketch 1.2

The hoses come out on top of the turbine casing next to the fixing of the rope and run along the rope down to turbine base. The tubes then have to cover at least a distance bigger than the operating range of the turbine on the seabed before reaching a second base, the so-called generator base. This base is then connected over a steel wire to the generator platform which is placed on the water surface. The hoses rise along the rope from the generator base to the platform.

At the platform the hoses run into a hydraulic motor which then drives the generator. There are two solutions to mount the base on the surface. The first one is, as I described, a floating platform which is fixed via a rope to the seabed. The rope needs to be at least as long as the water is deep at high tide. Therefore the platform will have some space to move at neap tide.

A second option is to install a massive concrete construction like an oil platform to secure motor and generator. This base would be placed slightly above sea level (~1-2m), enough to not be disturbed by rough sea state and to be easily accessible by boat.

The advantages over the free-floating system are that maintenance work can also be made in bad weather conditions and the possibility that devices are affected by strong sea is much smaller.

2. Turbine Design

2.1. Turbine theory

Predicting the performance of a counter-rotating turbine made it necessary to make certain assumptions. The two rotors function as a single actuator disc regarding blade element theory, because of their proximity.

Calculations, which were carried out by *J A Clarke, G Connor, A D Grant and C M Johnstone* of the *Energy Systems Research Unit* (ESRU) at *Strathclyde*, came to the conclusion that maximum efficiency is achieved, when the upstream rotor consists of 3 blades and the downstream rotor incorporates 4 blades. It is crucial that the torque on the two rotors is about same to get a zero reaction torque. To achieve this Furthermore, the *blade tip speed ratio* λ should be slightly higher for the upstream rotor in order to obtain a zero reaction torque.

Ω …..Rotor angular velocity
R…...Radius at blade tip
V…...Flow velocity

$$\lambda = \frac{\Omega \cdot R}{V}$$

Preceding tests, also executed by ESRU, with the 0.82 m diameter – prototype (see picture 1.4 on page 4) showed that the power coefficient reaches its highest value $c_P \approx 0.4$, when the tip speed ratio $\lambda \approx 7$.

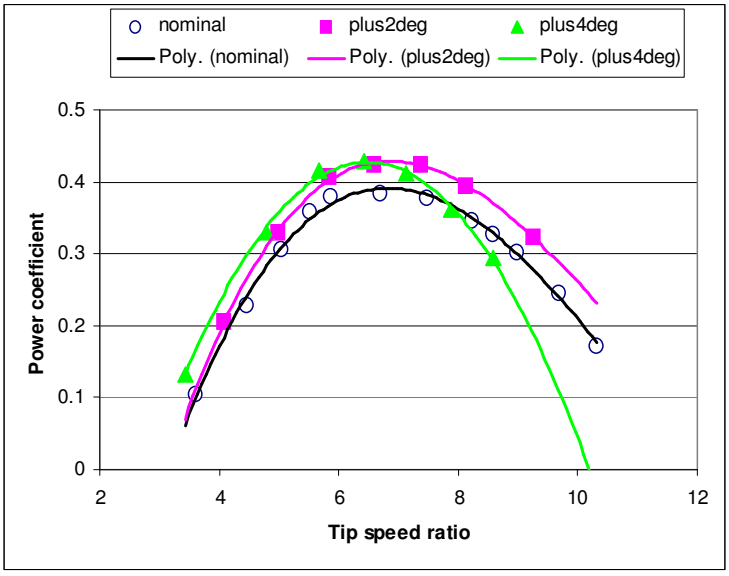

Diagram 2.1

Considering the fact that we have a counter-rotating turbine means that reasonable λ values for the up- and downstream turbine would be 3,5 respectively 3,4.

$$\lambda = \lambda_1 + \lambda_2 = 3{,}5 + 3{,}4 = 6{,}9$$

I investigated on a marine current turbine with a total rated power output of 300 kW. Around the western side of Scotland peak flows of 2.5 m/s are possible, so I took this value as my rated speed.

Furthermore, it is important to set a minimum speed level, the so-called cut-in speed, when the plant should start to operate. This depends mainly on the minimal input requirements of the different devices in the system. So I choose a cut-in speed of 0.75 m/s.

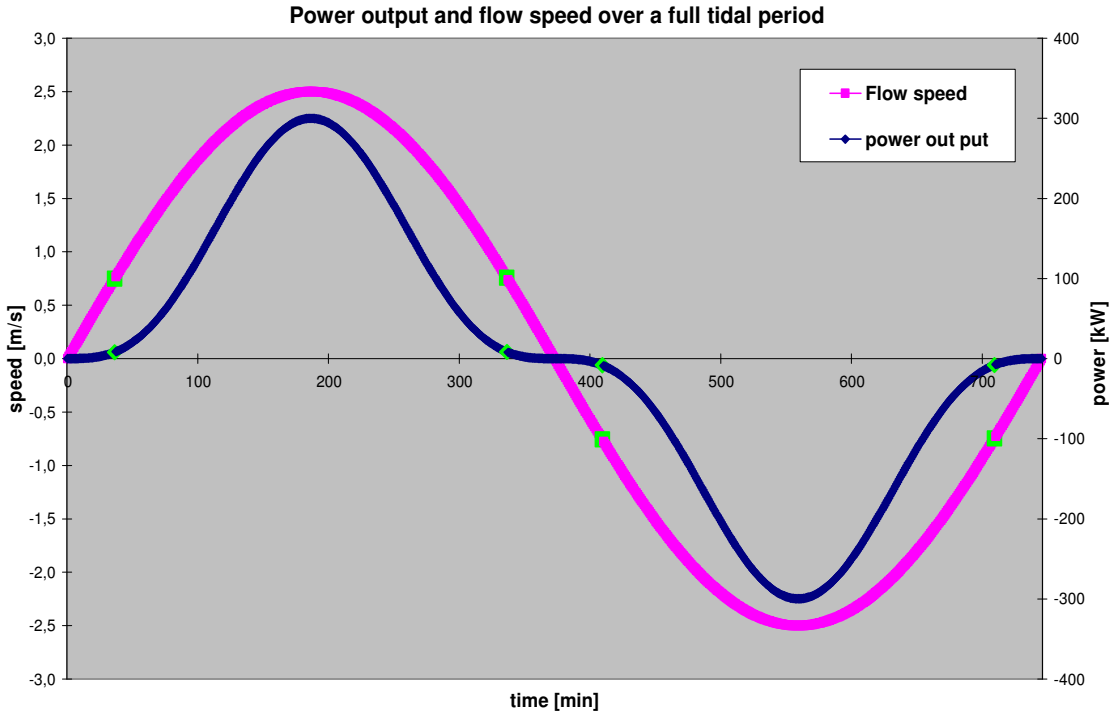

Diagram 2.2

2.2. Turbine specifications

Considering the tip speed ratio and the power output, I wanted to find the possible revolution speeds for the two rotors and their radiuses.

I took the data for the power efficiencies of the two rotors c_{P1} respectively c_{P2} from specification sheet of the 0.82 m - prototype. Taking the ratio of c_{P1} and c_{P2}, I could define the power each rotor actually produces.

$$c_{P1} = 0.2225 \qquad c_{P2} = 0.2116 \qquad \Rightarrow \qquad c_P = 0.4341$$

$\rho = 1025\ kg/m^3$

$V_R = 2.5\ m/s$

$$\frac{c_{P1}}{c_{P2}} = \frac{0.2225}{0.2116} = 1.052 \qquad \Rightarrow \qquad P = P_1 + P_2 = P_1 + P_1 \cdot 1.052 = 300kW$$

$\Rightarrow \underline{P_1 = 153.767\ kW}$

$\Rightarrow \underline{P_2 = 146.233\ kW}$

Turbine power: $$P = \frac{1}{2} \cdot c_P \cdot \rho_W \cdot \pi \cdot R^2 \cdot V^3$$

As I had P and c_P for both rotors, I could calculate their radiuses, which were of course the same.

$$\Rightarrow R_1 = \sqrt{\frac{P_1}{0.5 \cdot c_{P1} \cdot \rho_W \cdot \pi \cdot V_R^{\ 3}}} = \sqrt{\frac{153767}{0.5 \cdot 0.2225 \cdot 1025 \cdot \pi \cdot 2.5^3}} = \underline{\underline{5.306m}}$$

$$\Rightarrow R_2 = \sqrt{\frac{P_2}{0.5 \cdot c_{P2} \cdot \rho_W \cdot \pi \cdot V_R^{\ 3}}} = \sqrt{\frac{146233}{0.5 \cdot 0.2116 \cdot 1025 \cdot \pi \cdot 2.5^3}} = \underline{\underline{5.306m}}$$

Finally, I evaluated the revolution velocities of each rotor.

$$\lambda = \frac{\Omega \cdot R}{V} = \frac{2 \cdot \pi \cdot n \cdot R}{60 \cdot V}$$

$$n_{1R} = \frac{\lambda_1 \cdot V_R \cdot 60}{2 \cdot \pi \cdot R} = \frac{3.5 \cdot 2.5 \cdot 60}{2 \cdot \pi \cdot 5.306} = \underline{\underline{15.746}}$$

$$n_{2R} = \frac{\lambda_2 \cdot V_R \cdot 60}{2 \cdot \pi \cdot R} = \frac{3.4 \cdot 2.5 \cdot 60}{2 \cdot \pi \cdot 5.306} = \underline{\underline{15.297}}$$

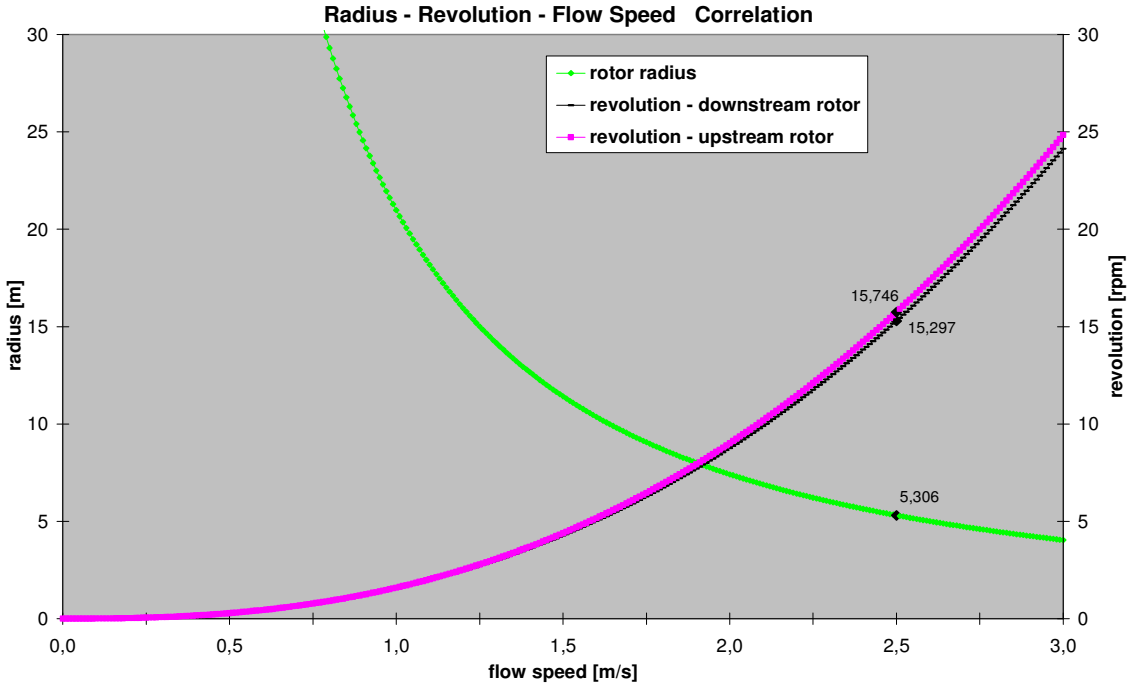

Diagram 2.3

The diagram shows the radius of the turbine and the revolutions of the rotors in relation to the flow speed of the water for a total power output of 300 kW. It is obvious that a high flow speed is crucial in order to keep the diameter of the rotors small. A bigger diameter could narrow the possible operational areas, for example in regions of shallow depth, because of the free-wheeling mounting of the turbine.

Moreover, bearing in mind a constant tip speed ratio, a larger diameter would cause a smaller revolution speed. This would be disadvantageous in our prototype system as we do not prefer to use a gearbox for efficiency respectively cost reasons.

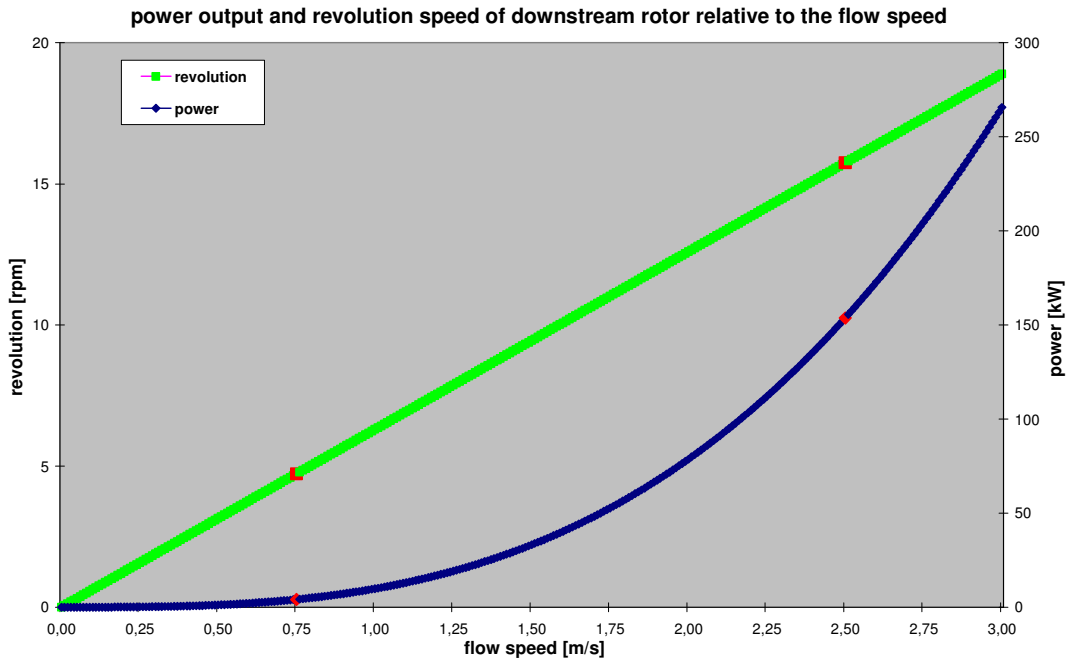

Diagram 2.4

3. Drive train design and specifications.

3.1. Pumps

Keeping the costs for each part low is crucial, so I only took serial-production devices into consideration. Firstly, it was important to find a hydraulic pump which meets the special requirements of a marine current turbine. The turbine produces all the power primarily with its high torque. We do not want to add two gearboxes to increase the rotational speed of the turbine. Whereas common and cheap *axial piston* or *gear* pumps are constructed to reach their rated power output at high revolution speeds (>2000rpm), we need a pump which is capable of transmitting all the power at an unusual low revolution speed of around 15 rpm. One characteristic feature of radial piston pumps is their capability of producing high pressure at low speeds.

3.1.1. Selecting pump model

The Swedish company *Hägglunds* produces marine motors. Their program of compact pumps is of the radial-piston type, where the cylinder block and hollow shaft is rotating and the housing is stationary. As it is shown in the picture, when rotation occurs, the cam rollers are gliding along the slope of the cam ring. The cam rollers transfer the pressure which works on them to the pistons which then produce the hydraulic pressure on flowing through oil. If necessary the compact CB can produce maximum torque from zero to maximum speed (all pictures and diagrams have been taken from *Hägglunds drives AB*).

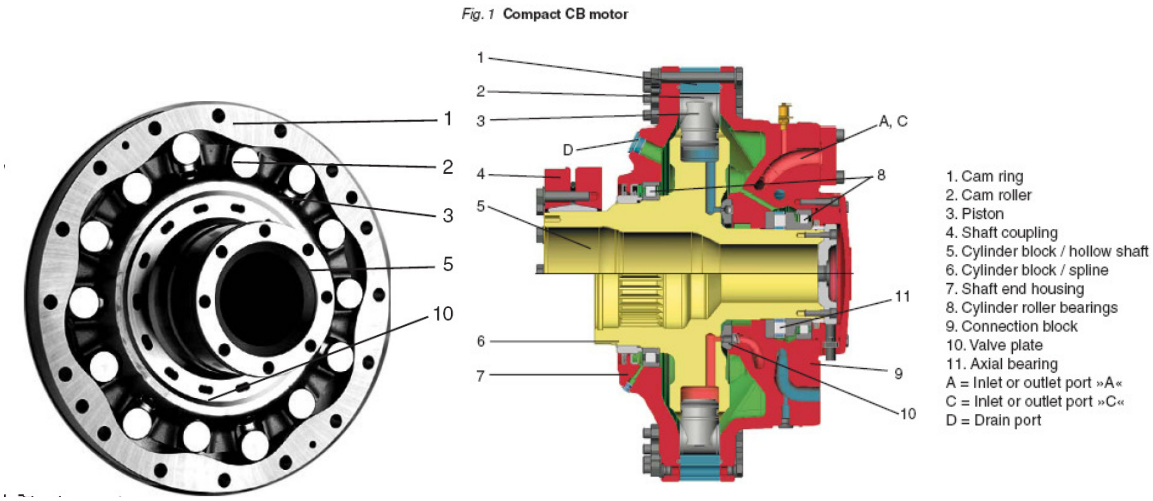

Pictures 3.1 & 3.2 - © Hagglünds

First of all, the pump should be able to transmit the high torque of the rotors. The torque at rated power is

$$T_{1R} = \frac{P_{1R}}{\Omega_{1R}} = \frac{153767}{2 \cdot \pi \cdot \frac{15.746}{60}} = \underline{\underline{93253.314 Nm}}$$

Torque at cut-in speed (0.75 m/s):

$$T_{1C} = \frac{P_{1C}}{\Omega_{1C}} = \frac{4151}{2 \cdot \pi \cdot \frac{4.724}{60}} = \underline{\underline{8391.010 Nm}}$$

The compact CB 400 can produce a maximum torque of 130 kNm and a maximum intermittent power of 970 kW which satisfies our needs by far as we would only need around 150 kW. However, the company suggests for a long term application to consider the CB 560 for a modified rating life of L_{10aah} = 40000 h and a charge pressure of P_C = 15 bar.

Selecting the right model:

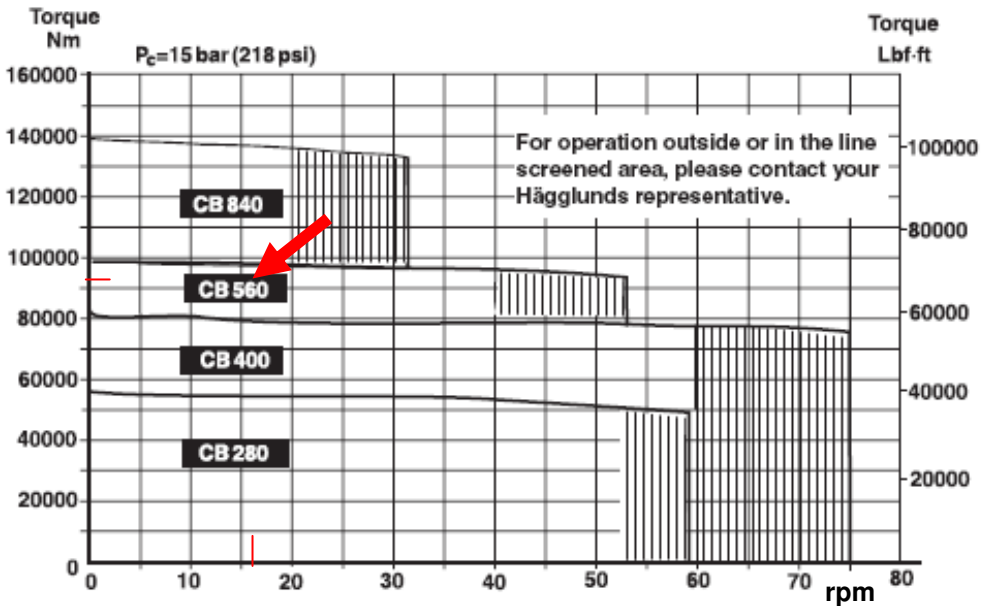

Diagram 3.1 - © Hagglünds

Motor data – Compact CB:

Metric Motor type	Displace-ment	Specific torque	Rated * speed 1)	Max. speed	Max. ** pressure	Max. torque 2)	Max. power 3) intermittently
	V_l cm³/rev	T_s Nm/bar	*n* rev/min	*n* rev/min	*p* bar	kNm	kW
CB 280-240	15 100	240	53	68	350	79	530
CB 280	17 600	280	44	58	350	92	530
CB 400-240	15 100	240	94	125	350	79	970
CB 400-280	17 600	280	73	105	350	92	950
CB 400-320	20 100	320	71	94	350	110	970
CB 400-360	22 600	360	59	82	350	120	960
CB 400	25 100	400	58	75	350	130	970
CB 560-440	27 600	440	49	65	350	140	930
CB 560-480	30 200	480	48	62	350	160	970
CB 560-520	32 700	520	41	57	350	170	960
CB 560	35 200	560	40	53	350	180	970
CB 840-600	37 700	600	30	45	350	200	880
CB 840-640	40 200	640	28	41	350	210	850
CB 840-680	42 700	680	27	40	350	220	890
CB 840-720	45 200	720	25	37	350	240	870
CB 840-760	47 800	760	23	34	350	250	840
CB 840-800	50 300	800	23	34	350	260	890
CB 840	52 800	840	21	32	350	280	870

Table 3.1 - © Hagglünds

I selected the CB 560-440 model as it fits better to the specifications of the chosen hydraulic motor. Then I calculated the hydraulic pressure output and the required volume flow rate.

3.1.2. Further pump specifications

3.1.2.1. Charge Pressure P_C (valid for a case pressure of 1 bar)

The recommended charge pressure is shown in diagram 3.2 below. The low-pressure port has to be fed with sufficient charge pressure which is in this case 3 bar for around 16 rpm.

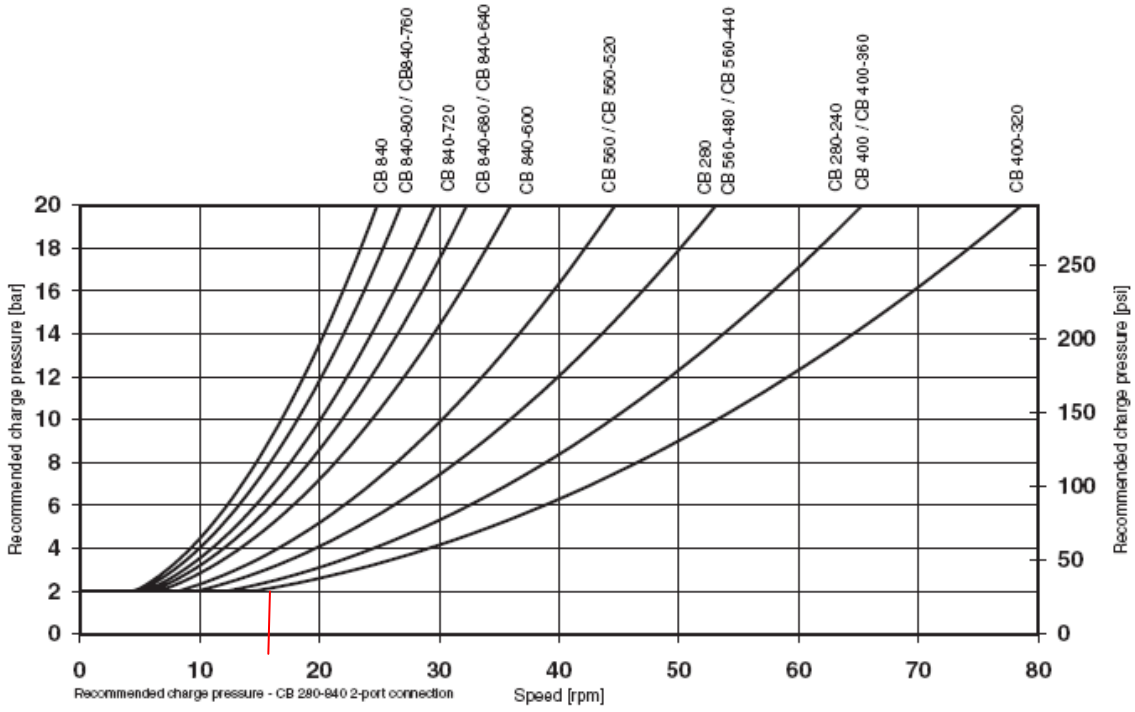

Diagram 3.2 – © Hagglünds

3.1.2.2. Pressure loss Δp_L

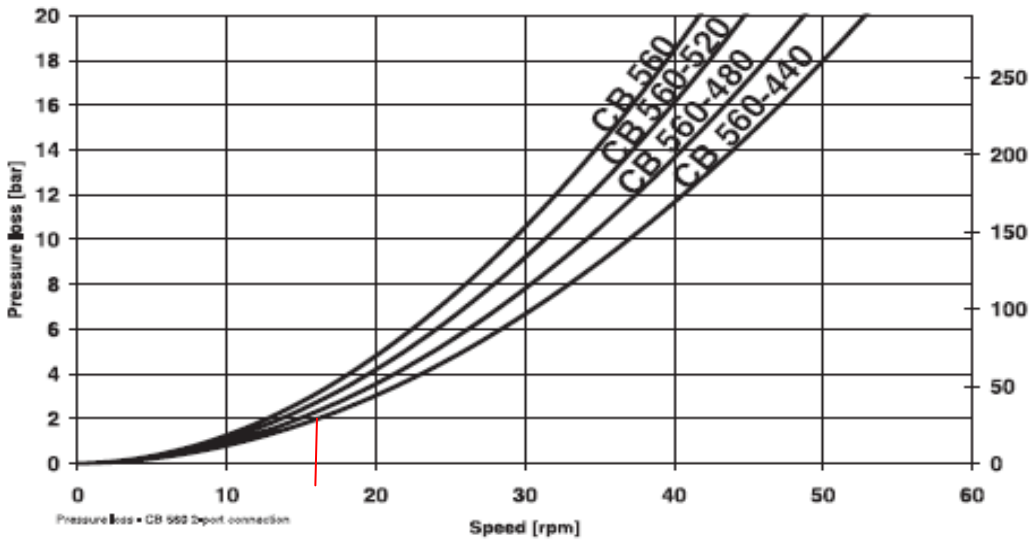

Diagram 3.3 – © Hagglünds

Mechanical efficiency $\eta_m = 0.98$

At rated speed: $$p_{1R} = \frac{T_{1R}}{T_S \cdot \eta_m} + \Lambda p_L + P_C = \frac{93253.314}{440 \cdot 0.98} + 2 + 3 = \underline{\underline{221.264 bar}}$$

At cut-in speed: $$p_{1C} = \frac{T_{1C}}{T_S \cdot \eta_m} + \Lambda p_L + P_C = \frac{8391.010}{440 \cdot 0.98} + 0 + 2 = \underline{\underline{21.460 bar}}$$

3.1.2.3. Flow rate q

Volumetric losses q_L (valid for a viscosity of 40 centistokes):

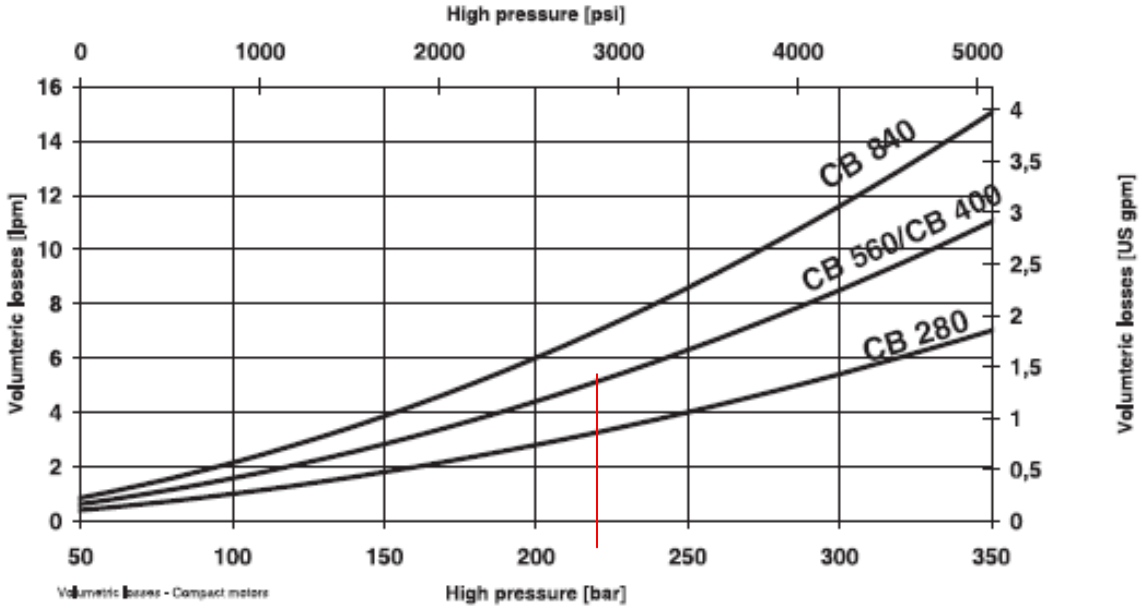

Diagram 3.4 – © Hagglünds

At rated speed: $$q_R = \frac{n_{1R} \cdot V_i}{1000} + q_L = \frac{15.746 \cdot 27600}{1000} + 5 = \underline{\underline{439.590 l/\min}}$$

At cut-in speed: $$q_C = \frac{n_{1C} \cdot V_i}{1000} + q_L = \frac{4.724 \cdot 27600}{1000} + 1 = \underline{\underline{131.382 l/\min}}$$

3.1.3. Hydraulic oil requirements

As Hägglunds motors are able to work with conventional petroleum-based hydraulic oils, so it is mainly important to choose the right oil viscosity. Either too low or too high viscosity leads to a reduced life expectancy and moreover to a reduction of maximum power output. Operating temperature should be lower than 50°C, which should be unproblematic, as the pump operates in the sea at around 5-10 °C. The water content in the hoses should not exceed 0.05%. Generally, the recommended kinematic viscosity at operating temperature should be between 40-150 cSt (1 centistoke = 1 mm^2/s) respectively 187 – 200 SSU (Saybolt Universal Seconds).

Furthermore, the hydraulic fluid has to be harmless in environmental concerns yet service life should be comparably equal to mineral oil. Synthetic ester HE is an environmentally approved hydraulic fluid and has the advantage over vegetable fluid HTG that it does not need to be controlled in such short intervals (3 months). HE oils have very good viscosity and lubricity, they are good protection against corrosion and are very easy degradable.

As short service intervals increase the costs in a significant way, especially in case of a marine current turbine, it is well recommended to consider a high grade of filtration. Hägglunds suggests a grade of filtration ß10=75, which means that 75% of all particles bigger than 10µm are filtered.

3.1.4. Pump efficiency

The pump will work, considering the specifications of the turbine, approximately inside the 94-95% area for most of time. The red pointer shows in the diagram 3.5 (below) approximately the pump's efficiency at rated power output and the red dot marks the place of highest efficiency.

Overall efficiency (red marks stand for rated values):

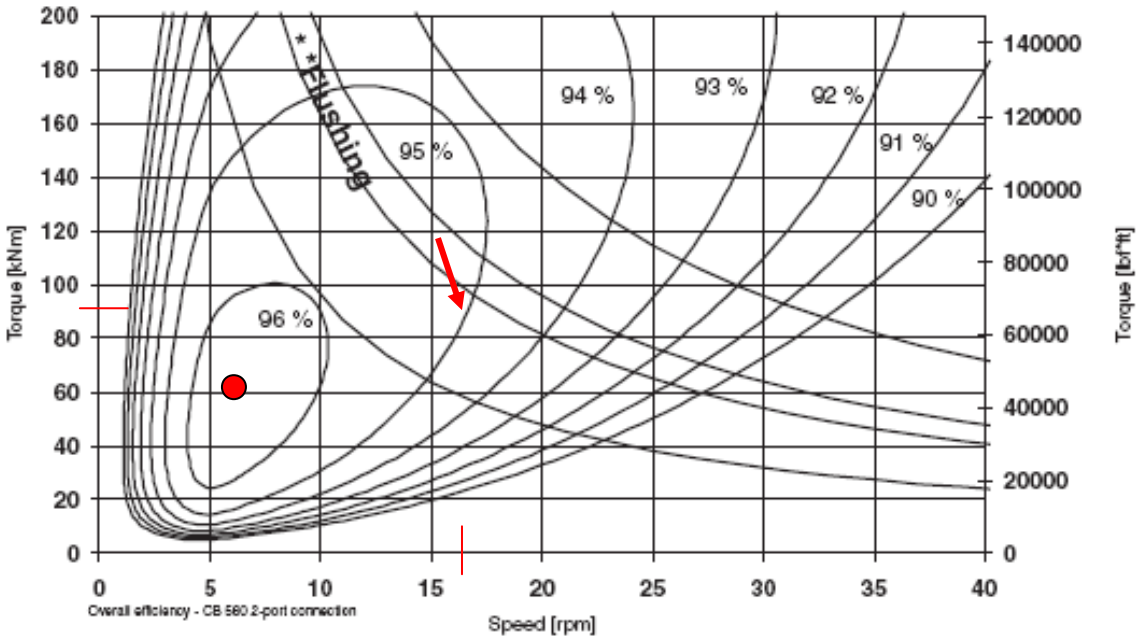

Diagram 3.5 – © Hagglünds

Flushing of the compact CB will not be required as the maximum permitting power of 170 kW will not be reached.

The price for each pump is around 12000£, which sums up to 24000£ for both.

3.2. Hydraulic motor – generator combination options

There are many different possible constellations and ways to transmit power from the motor the generator, yet finding the most economic is the priority. Although, marine current turbines are working in a completely different environment than wind turbines, there are still some similarities. As the wind power economy is far ahead of the tidal power economy, some of their solutions might also succeed in the tidal power market.

The problem with wind turbines, even more than with marine current turbines, is their huge speed variability. This fact has forced companies to use more sophisticated generator systems to improve the overall efficiency.

Nowadays there are mainly 4 generator systems in use (see pictures 3.3 – 3.6; all graphics have been taken from *Siemens AG*). Depending on the power output of the turbine asynchronous or synchronous generators are preferred. For smaller constructions a fixed speed generator system consisting of an induction generator (squirrel cage) and a gearbox are favoured because of its simplicity, reliability and cheapness.

However, the generator will not run all the time highly efficient as the speed alterations of the wind cannot be completely adjusted by the gearbox for its fixed ratios. The necessity of keeping the frequency at 50 Hz makes the generator slip the only tuneable variable which causes losses due to high reactive currents. Nevertheless, for small scale solutions this system is still the best option.

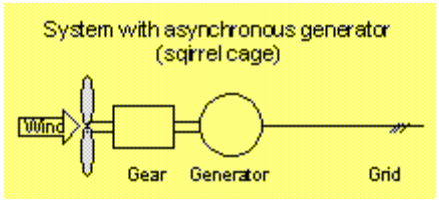

Picture 3.3 © Siemens AG

Variable speed generator systems are widely used nowadays in bigger wind farms, because of their higher efficiency and controllability. The most common constellation is a double fed slipring generator whereas the speed is controlled over rotor circuit and the converter only has deal with the slip power.

Another solution is connecting a separately excited synchronous generator with an inverter and a gearbox. The advantages are controllability of the reactive power, high efficiency, high reliability and low maintenance costs.

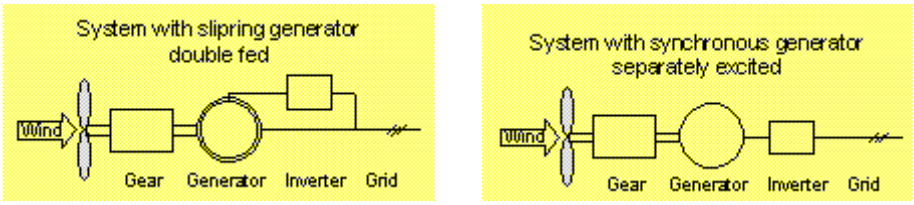

Pictures 3.4 & 3.5 © Siemens AG

Gearless systems are especially interesting for offshore devices as these achieve the highest level of efficiency. The consequences of omitting the gearbox are higher efficiency due to no gear losses and lower maintenance costs as there are less devices involves in the application. Moreover, synchronous generators are more reliable than slipring generators and have higher mechanical load capacity.

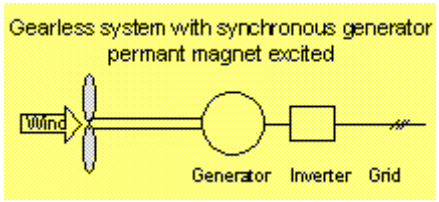

Picture 3.6 © Siemens AG

In my case study, I have a hydraulic connection from the turbine to the generator which makes the approach different to the 4 constellations described above.

One possibility is to link the hoses to a normal hydraulic motor and connect the motor then to a gearbox which is on its part connected to a squirrel cage generator like it is shown in the first type above. However, connecting 3 devices together raises acquisition and maintenance costs and decreases efficiency due to higher transmission losses. That is why I considered to omit the gearbox and to take a hydraulic motor with a variable displacement. It should impel the generator with a constant speed in order to keep up a constant frequency of 50 Hz. Considering a suitable hydraulic motor runs around 2000 rpm, a generator with 2 pole pairs is nearly ideal as it produces a net frequency of 50 Hz at 1500 rpm.

3.3. Hydraulic motor specifications

The company Rexroth, a subsidiary of the Bosch group, is a supplier of a variety of hydraulic products. The A6VM is an axial piston hydraulic motor with the possibility of varying the displacement. The hoses of both pumps will be connected so that the volume flow doubles.

Rated volume flow: $q_{total,R} = 2 * q_R = 2 * 439{,}590 = \underline{\underline{879{,}180 \ {}^{l}/_{min}}}$

Cut-in volume flow: $q_{total,C} = 2 * q_C = 2 * 131.382 = \underline{\underline{262.765 \ {}^{l}/_{min}}}$

Commend: Simplification, as downstream pump produces a few percent less volume flow than upstream pump.

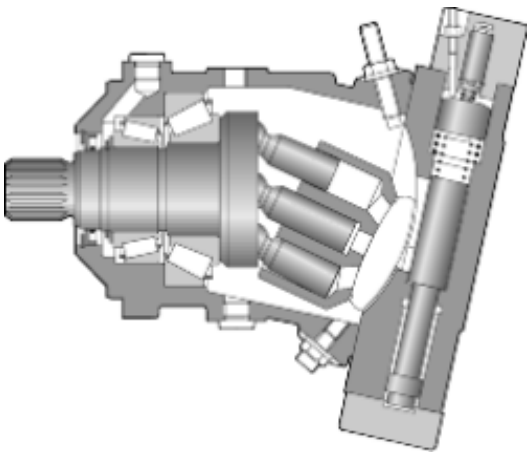

Pictures 3.7 & 3.8 © Bosch - Rexroth

Specification sheet:

Size				28	55	80	107	140	160	200
Displacement		**$V_{g\,max}$**	**cm^3**	28,1	54,8	80	107	140	160	200
Speed (maintaining q_{Vmax})	**at $V_{g\,max}$**	**n_{max}**	**min^{-1}**	5550	4450	3900	3550	3250	3100	2900
	at $V_g < V_{g.1}$	**n_{max}**	**min^{-1}**	8750	7000	6150	5600	5150	4900	4600
		$V_{g.1}$	**cm^3**	18	35	51	68	88	101	126
Input flow	**at n_{max}**	**q_{Vmax}**	**L/min**	156	244	312	380	455	496	580
Power	**Δp= 400bar**	**P_{max}**	**kW**	104	163	208	253	303	331	387
Torque	**Δp= 400bar**	**T_{max}**	**Nm**	179	349	509	681	891	1019	1273
Weight (approx.)		**m**	**kg**	16	26	34	47	60	64	80

Size				250	355	500	1000
Displacement		$V_{g\,max}$	cm^3	250	355	500	1000
Speed (maintaining q_{Vmax})	**at $V_{g\,max}$**	n_{max}	min^{-1}	2700	2240	2000	1600
	at $V_g < V_{g.1}$	n_{max}	min^{-1}	3600	2950	2650	2100
		$V_{g.1}$	cm^3	190	270	385	762
Input flow	**at n_{max}**	q_{Vmax}	**L/min**	675	795	1000	1600
Power	**Δp= 350bar**	P_{max}	**kW**	394	464	583	933
Torque	**Δp= 350bar**	T_{max}	**Nm**	1391	1978	2785	5571
Weight (approx.)		**m**	**kg**	90	170	210	430

Table 3.2 - © Bosch-Rexroth

The A6VM - size 500 has a maximum volume flow of 1000 l/min at 2000 rpm, which means that at the required revolution speed of 1500 rpm the maximum flow measures 750 l/min. As this is significantly below 880 l/min, I have to opt for the biggest available device in the portfolio, the A6VM-1000, whose maximum power output of 933 kW is well over the system's rated capacity. A hydraulic motor supplied by Bosch with these dimensions costs at least 17000 £.

The displacement at the aimed generator speed of 1500 rpm is

At rated speed: $$V_{D,R} = \frac{q_{total,R}}{n_G} = \frac{879.180 * 1000}{1500} = \underline{\underline{586.120 cm^3}} = 0.586 * V_{g\,max}$$

At cut-in speed: $$V_{D,C} = \frac{q_{total,C}}{n_G} = \frac{262.765 * 1000}{1500} = \underline{\underline{175.177 cm^3}} = 0.175 * V_{g\,max}$$

The full displacement of the A6VM-1000 is 1000 cm³. The displacement shift from cut-in to rated speed is

$$\Delta V = 586.120 - 175.177 = \underline{\underline{410.943 cm^3}}$$

The standard displacement setting of the hydraulic motor is from V = 0.2*V_{max} to V = V_{max}, which means that the displacement at cut-in speed is slightly too low, however it is possible to preset the displacement shift regarding to the specific requirements. The motor has a nominal pressure of 350 bar and can withstand possible peak pressures of 400 bar, which is well over the rated pressure of 221 bar coming from the turbine. So a long-life cycle can be expected.

3.3.1. Further hydraulic motor specifications

Case pressure should be at least as big as the external pressure on the shaft seal ring. The drain pressure at continuous operation should be not higher than 3 bar, because exceedance will shorten life expectancy. The diagram below shows the permissible pressure trends. At 1500 rpm the value is around 3.4 bar for the A6VM-1000.

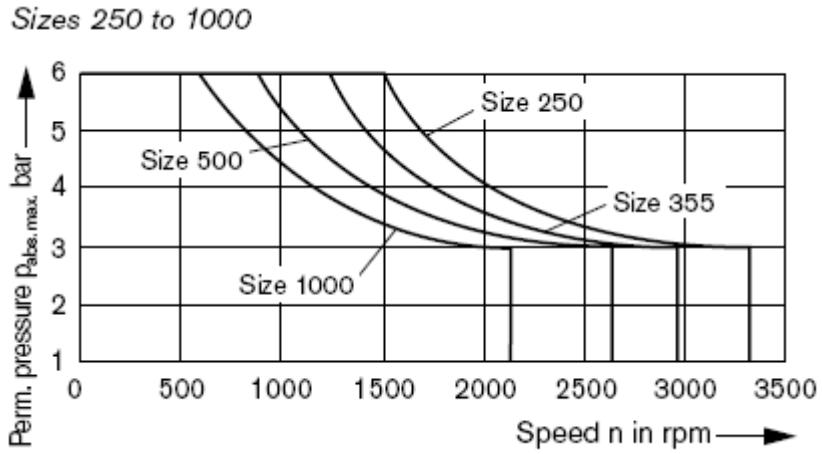

Diagram 3.6 – © Bosch-Rexroth

The minimum inlet pressure should not fall below the limits shown in the diagram below. This should not be problematic, because the minimum cut-in pressure is around 21 bar and critical values start well below 7 bar (see diagram 3.7)

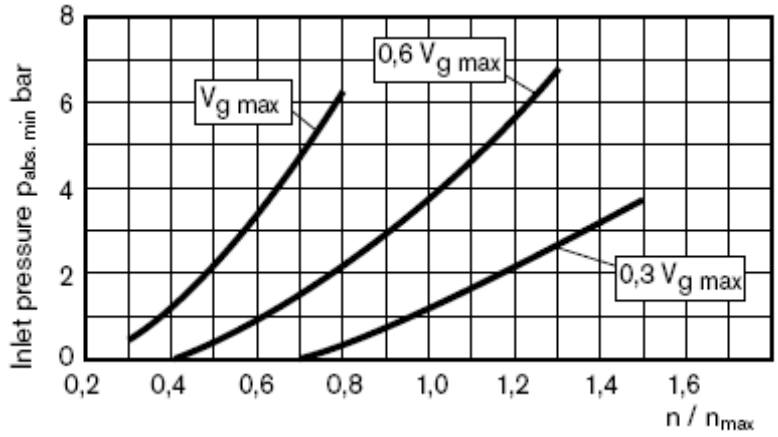

Diagram 3.7 – © Bosch-Rexroth

3.3.2. Flushing

The motor accommodates a flush and boost pressure valve. Its purpose is removing heat from circuit and guaranteeing minimum boost pressure, but also to flush the case and cool the system down. Flushing of bearing is also recommended. Flushing volume for the A6VM – 500 is 16 l/min.

3.3.3. Oil selection

Bosch-Rexroth suggests oil with an operating viscosity between 16-36 mm²/s. The viscosity limits are between 10 and 1000 mm²/s, whereas though a viscosity between 16 and 100 mm²/s is necessary to ensure 100% functionality and lifetime (*reference 15*).

viscosity	time	temperature	pressure	rev. speed
10 mm²/s	< 3 min.	T < 90°C	-----	-----
1000 mm²/s	< 3 min.	T > -25°C	p < 30 bar	n < 1000rpm

Table 3.3 – © Bosch-Rexroth

Getting the right oil which fulfils all the requirements of the overall system is a compromise. First of all, Hägglunds suggests viscosity limits from 40 - 150 mm²/s, which is slightly above the Bosch optimum values of 16-36 mm²/s. An oil viscosity from 50 to 100mm²/s is preferable, because it is better to keep the viscosity value a little higher in order to avoid damages.

The use of hydraulic fluids based on esters – type HEE – is permissible like in the Hägglunds drives. There are four possible oil viscosities available, as it is shown in the diagram below, the VG 22/32/46/68. The number stands for the viscosity in mm²/s at 40°C.

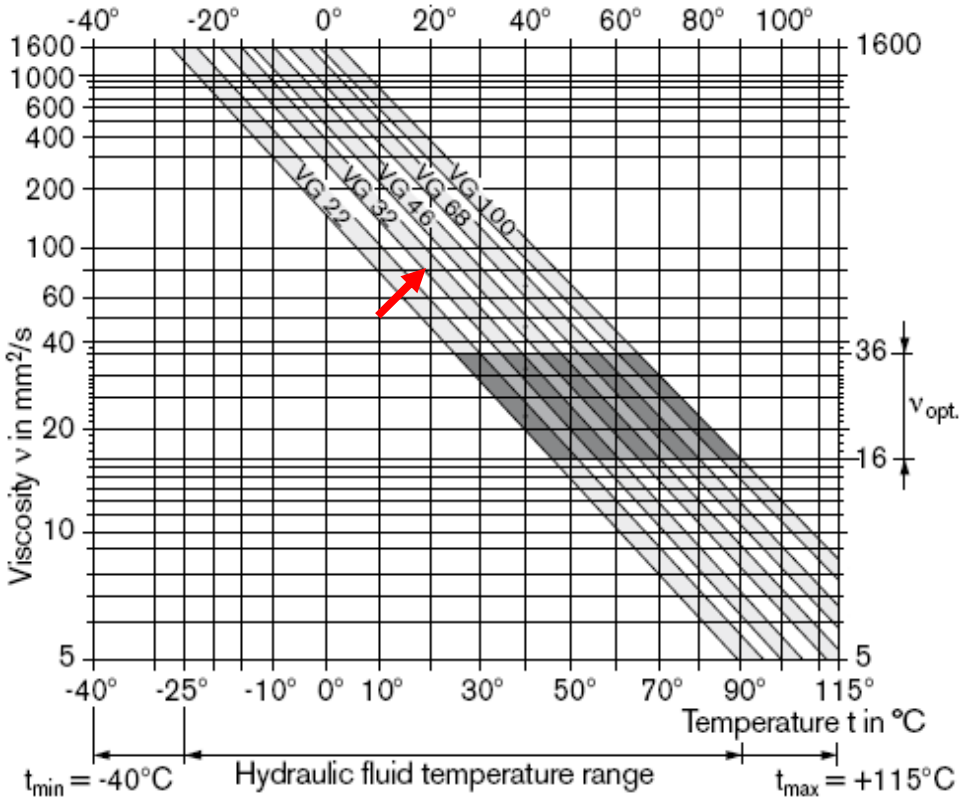

Diagram 3.8 – © Bosch-Rexroth

Considering the hoses are mostly underwater, the temperature of the oil will not be very high, because of the cooling effect of the sea. The sea temperature in Scotland approximately between 5 and 15 °C on average which means that, based on estimate, the oil temperature will be not so much higher as hoses lay a hundred meters each in water. Still, frictions losses will have an opposite effect.

Fluids of the viscosity class VG 32 have a viscosity of around 80mm²/s at 20°C. If operating temperature is not lower, this oil should suit quite well. Nevertheless, this needs to be further tested and investigated because the oil quality and specification has a big impact on life-cycle, service intervals and efficiency.

The filtration quality is specified by the ISO 4406 standard – class 18/15 which is as demanding as Hägglunds' specifications (class 19/15). Each class number defines the maximum number of particles allowed at a certain size. In this case, class 18 means up to 250000 particles bigger than 6µm and class 15 means up to 32000 particles bigger than 14µm.

3.3.4. Service intervals

One major problem of the whole hydraulic drive solution is the short service intervals due to the necessary change of the hydraulic fluid. Bosch recommends an oil change every 2000 hours respectively one time per year if the machine is not used all the time. Hägglunds suggests an oil inspection and filter change at least every 6 months.

At high usage level, oil tends to become thinner and the lubrication gets worse. The oil is also exposed to oxidation processes, which increase its acidity. It can rapidly increase and lead to damage. Other quality reducing factors are increase of water content and contamination. All this factors wear down the machines and decrease life circle.

In an offshore system, where large maintenance intervals are essential, it is not ideal to have operating devices which need continuous inspections, even more if this causes cuts in power supply.

3.3.5. Controlling

The minimum suggested pressure and volume flow for a reliable control are 30 bar respectively 20% of the maximum volume flow, which is 200 l/min. These requirements are a little over the cut-in specifications, which means that maybe the cut-in/out speed needs to be increased. A cut-in speed of 0.9 m/s would lift the pressure and the flow above the minimum demand. However, this would lead to a power production loss and needs further consideration. Still, at 0.9 m/s the power output is 14 kW, less than 5% of the rated power.
All control mechanisms are capable of varying speed and pressure of the system. The displacement shift is made by variation of the pilot-pressure. A full displacement shift means a pilot-pressure difference of 10, 25 or 35 bar depending which characteristic curve is programmed.

3.4. Generator specifications

Omitting the gearbox in favour of a - yet more expensive – fully variable displacement, hydraulic motor has the positive consequence that the generator can always be driven at a constant speed of 1500 rpm. The power efficiency will not be badly affected by fixed gear transmission ratios.

Siemens has a range of generators which are especially produced for the on/off - shore wind farm market. Their single-speed, 4-pole squirrel cage generators develop between 30 and 5000 kW. As the optimum generator slip is about 1%, the generator will run at 1515 rpm at rated power.

Picture 3.9 © Siemens

cooling method	self ventilation IC 411, alt. forced ventilation IC 416		alt. air/air- or air/water-cooler
voltage	3 AC 400 V / 500 V / 690 V	up to 11 kV	
power	30 - 1900 kW	200 - 3000 kW	1000 - 5000 kW
shaft height	250 - 560	355 - 630	450 – 560
degree of protection	IP55		

Table 3.4 - © Siemens

I suggest a voltage level of 690 V because it is commonly used for off-shore applications.

Ampere level: $$I = \frac{P}{U} = \frac{300kVA}{690V} = \underline{\underline{435A}}$$

The price for a 300 kW generator is about 12000 £.

3.5. Hoses

3.5.1. Dimension requirements

Another point regards the connection between the hydraulic pump which is situated under the water and the hydraulic motor at the generator. The hoses must be capable to withstand the high pressure and to transport the volume flow at rated power.

Viscosity: 50 - 100mm²/s = 0.5 - 1 cm²/s
Cut-in pressure: 21.460 bar
Rated pressure: 221.264 bar
Cut-in volume flow: 175.177 l/min = 2920 cm³/s
Rated volume flow: 879.180 l/min = 14653 cm³/s

I looked for a high-pressure hose with a big diameter in order to decrease the flow speed. As a matter of fact doubling the diameter increases the wall thickness by a factor 8. Consequently, hoses which are built for a working pressure of around 200bar have usually at best an inner diameter of 2 inch (51 mm), whereas for this size 6 steel reinforcement layers are needed.

In order to be able to calculate the necessary diameter of the hose, I choose to take the turbulence of the flow as a reference. My reference value is the critical *Reynolds-number* of 2300, which marks the transition between laminar and turbulent flows. This however turns out to be a problematic point of this power connection, because hoses, which can meet our requirements, are rare or even non-existent as I will refer in the next pages.

First, I calculate the minimum diameter.

$$q_{total,R} = u \cdot A = u \cdot \frac{d^2 \cdot \pi}{4}$$

$$\mathrm{Re} = \frac{u \cdot d}{\nu} = \frac{q_{total,R}}{\frac{d^2 \cdot \pi}{4}} \cdot \frac{d}{\upsilon} = \frac{4 \cdot q_{total,R}}{d \cdot \pi \cdot \upsilon}$$

$$d = \frac{4 \cdot q_{total,R}}{\mathrm{Re} \cdot \pi \cdot \nu} = \frac{4 \cdot 14653}{2300 \cdot \pi \cdot 1} = \underline{\underline{8.112cm}}$$

3.5.2. Selecting hose model

The biggest standard hose I could find is the 'Diamond Spir' form the company *Manuli-Hydraulics* based in Italy. It is a wire-spiralled reinforced hose with 6 steel belts. The biggest diameter, as shown in the table below, is 76.2 mm = 7.62 cm, which is slightly below the preferred value, but still a considerable size. Burst pressure is 870bar which is way above the rated pressure. Furthermore, the hoses are built especially for heavy duty environmental conditions and they feature a high abrasion resistance. Abrasion protection is a significant aspect, because the hoses will partly lie on the seabed which might be rocky.

Picture 3.10 © Manuli-Hydraulics

HOSE SIZE			R.O.D.	O.D.	MAX. W.P.	BURST PRESS.	MIN BEND RADIUS	WEIGHT	FERRULE
DN	dash	mm	mm	mm	bar	bar	mm	g/m	
25	16	25,4	38,2	41,2	552	2.210	350	2.895	M01800-16
31	20	31,8	47,7	51,9	525	2.100	420	4.330	M01800-20
38	24	38,1	55,2	59,1	475	1.900	500	5.295	M01800-24
51	32	50,8	68,4	72,0	420	1.680	600	6.725	M01800-32
63	40	63,5	82,8	87,6	350	1.400	800	9.015	M01800-40
76	48	76,2	90,8	94,8	210	870	900	8.000	M01800-48

Table 3.5 - © Manuli-Hydraulics (red: selected model)

3.5.2.1. Defining turbulence in hose

Cut-in speed: $$u = \frac{q_{total,C}}{A} = \frac{q_{total,C}}{\frac{d^2 \cdot \pi}{4}} = \frac{2920}{\frac{7.62^2 \cdot \pi}{4}} = \underline{\underline{64.030 cm/s = 0.640 m/s}}$$

$$\mathrm{Re} = \frac{u \cdot d}{\nu} = \frac{64.030 \cdot 7.62}{1} = \underline{\underline{487.090}}$$

Rated speed: $$u = \frac{q_{total,R}}{A} = \frac{q_{total,R}}{\frac{d^2 \cdot \pi}{4}} = \frac{14653}{\frac{7.62^2 \cdot \pi}{4}} = \underline{\underline{321.312 cm/s = 3.213 m/s}}$$

$$\mathrm{Re} = \frac{u \cdot d}{\nu} = \frac{321.312 \cdot 7.62}{1} = \underline{\underline{2448.397}}$$

In calculations above I used the highest value (1 cm²/s = 100m²/s) in the kinematic viscosity range which I defined in the previous chapter (50 – 100 mm²/s). Keeping the Reynolds number as small as possible and consequently decrease the stream's turbulence is crucial to not lose power.

Although the Reynolds number is above the crucial mark of 2300, there is possibility that the flow is still not turbulent. When the flow speed is increased at a steady and slow pace the stream can still be laminar, theoretically up a Reynolds number of 40000 (*reference 28*).

Nevertheless, a further turbulence reduction is favourable. However, as I there are no bigger hoses for this high-pressure application available, purchasing a special designed hose off batch-production will lift the price remarkably. (If in future this kind tidal power system is well-established, the costs will of course decrease.)

3.5.2.2. Expenses

The price per meter of the 76 mm *Diamond Spir* is 57 £. When we estimate a realistic length of around 100 meters per hose, then we have an overall of 400 meters. That adds up to 22800 £, which is a quite considerable sum and for example more expensive than the generator.

3.5.2.3. Other issues

The friction losses in the hoses are worth a second thought. The level of turbulence and the length of hose system could reduce efficiency significantly. Further investigations on this topic are recommendable.

The two incoming hoses of the hydraulic motor need to be connected respectively the outgoing hose needs to be split up in two. Availability of fittings is questionable.

4. Power plant design

4.1. Turbine

4.1.1. Buoyancy

The buoyancy of the turbine is a crucial and critical issue. As I mentioned above the turbine should swing back and forth depending on the tidal current's direction. In order to achieve this we need to place an air tank into the turbine casing. Obviously a turbine with a high buoyancy force will stay in a vertical position at zero current speed and will also be far from horizontal at low speed. For efficiency reasons it is necessary that the turbine nearly always points towards the stream.

We have two forces impacting on the turbine: The drag force which increases exponential, whereas the buoyancy force remains constant. The drag force works normal to the buoyancy force. However, it pushes the turbine down the higher the flow speed is, because of the seabed mounting.

On one hand, we need strong buoyancy for keeping the turbine floating at any speed and for achieving the pendulum effect. Keeping the turbine away from seabed is the most important concern. Therefore, the buoyancy force should be at least as big as the drag force at rated speed in order to secure the turbine. Consequently, the resulting angle of the rope would be 45°.

On the other hand, strong buoyancy means that the turbine will never be 100% horizontal, not even at rated speed, which leads to a significant loss of power output.

4.1.2. Turbine base construction: method 1

One possible solution to this dilemma is placing the air tank at the front end of the turbine casing and decentralise the rope fixation on the turbine.

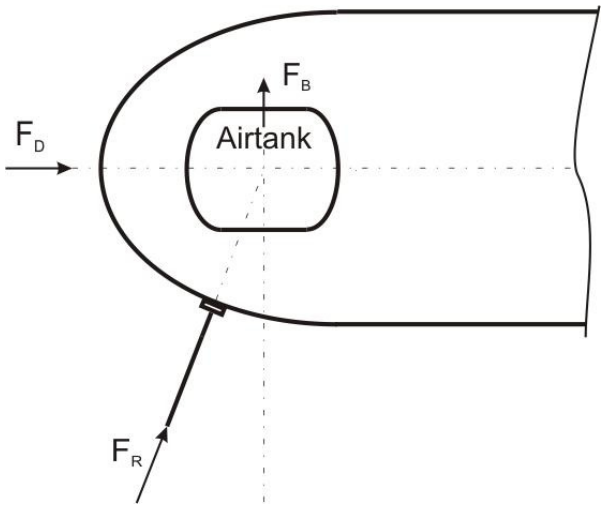

Sketch 4.1

The exact place of the rope mount and the air volume are the significant variables and small changes will lead to changes in the horizontal position of the turbine.
An acceptable compromise would be to achieve a horizontal turbine position (zero angle) at medium drag force for minimising deflection at low and high speed. Ideally, the turbine has the same horizontal angle at cut-in (positive angle) and rated speed (negative angle).

4.1.2.1.Drag force of turbine

First, we have to calculate the drag force of the turbine.

$C_D = 8/9$
$\rho_W = 1025$ kg/m³
$R = 5.306$ m

Drag force at cut-in speed $V_C = 0.75$ m/s:

$$F_{D,C} = c_D \cdot \frac{1}{2} \cdot \rho_W \cdot R^2 \cdot \pi \cdot V_C{}^2 = \frac{8}{9} \cdot \frac{1}{2} \cdot 1025 \cdot 5.306^{\cdot 2} \pi \cdot 0.75^2 = \underline{\underline{22.665kN}}$$

Drag force at rated speed $V_R = 2.5$ m/s:

$$F_{D,R} = c_D \cdot \frac{1}{2} \cdot \rho_W \cdot R^2 \cdot \pi \cdot V_R{}^2 = \frac{8}{9} \cdot \frac{1}{2} \cdot 1025 \cdot 5.306^2 \cdot \pi \cdot 2.5^2 = \underline{\underline{251.829kN}}$$

The drag force at rated speed is about 11 times bigger than at cut-in speed. So the angle α, which defines the position of the rope relative to the vertical axis, will vary significantly during a tidal period. The angle difference depends mainly on the buoyant force.

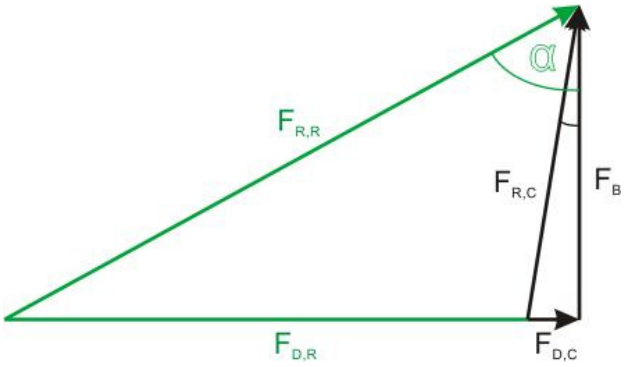

Sketch 4.2

4.1.2.2.Horizontal angle of turbine

Horizontal angle of the turbine according to changes in buoyancy and flow speed:

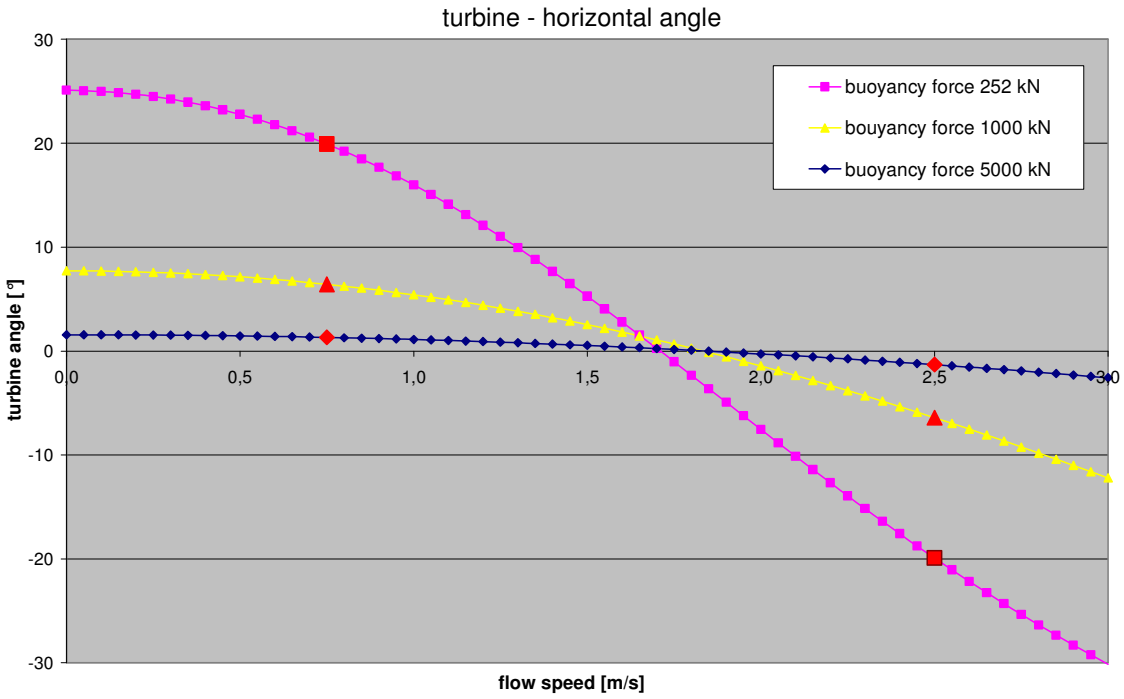

Diagram 4.1

Diagram 4.1 shows how angle of the longitudinal axle of the turbine changes over speed for three voluntary chosen buoyancy forces. The angle at cut-in speed and rated speed is the same. For comparing reasons, the smallest buoyancy force equals the rated drag force.

The higher the buoyancy, the higher is the speed where the turbine is horizontal (zero angle). More importantly, the higher the buoyancy the smaller gets the angular deflection on both ends, because the drag force gets smaller relative to the buoyancy. As a consequence, very high buoyancy is definitely preferable as this would limit the losses to some extend. However, even a buoyancy force of 1 MN causes a maximum angle of more than 6° and is far from optimal as also large amounts of air will be required.

There might be the possibility to realise a speed-related, longitudinal adjustable rope mounting in order to insure a 100% stabilised turbine, but this would lead to an increase of cost and complexity.

In perspective of a high efficiency, I define a maximum deflection of 5° for the longitudinal axis of the turbine. The effects, like the reduction of the working surface, the angle has on the drag force and the power output needs to be investigated.

Corrected drag force at rated speed:

$$F_{D,R,c} = c_D \cdot \frac{1}{2} \cdot \rho_W \cdot \cos\alpha \cdot R^2 \cdot \pi \cdot V_R{}^2 = \frac{8}{9} \cdot \frac{1}{2} \cdot 1025 \cdot \cos 5° \cdot 5.306 \cdot \pi \cdot 2.5^2 = \underline{\underline{250.871 kN}}$$

Compared to the original drag force (page 43) the real drag force is nearly the same (99.6%). That percentage also applies for the overall power output.

I assume from the diagram above a buoyant force of 1500 kN to be well within the 5° limit.

Angle at cut-in speed: $\arctan\left(\frac{F_{D,C}}{F_B}\right) = \arctan\left(\frac{22.665}{1500}\right) = 0.866°$

Angle at rated speed: $\arctan\left(\frac{F_{D,R}}{F_B}\right) = \arctan\left(\frac{250.871}{1500}\right) = 9.495°$

Proof of equal angles:

Maximum angle at cut-in speed: $\frac{9.495 + 0.866}{2} - 0.866 = \underline{\underline{4.316}}$

Maximum angle at rated speed: $\frac{9.495 + 0.866}{2} - 9.495 = \underline{\underline{-4.316}}$

4.1.2.3. Air tank volume

Buoyant force: $F_B = \rho_W \cdot V_B \cdot g$

1500 kN buoyant force leads to a required air volume of approximately 150 m³. For calculating the required dimensions of the air container, I assume a cylindrical shape, because this geometry fits best in the turbine casing and a cylinder length of 10 meters.

$$V_B = r_B{}^2 \cdot \pi \cdot h_B \qquad => \qquad r_B = \left(\frac{V_B}{\pi \cdot h_B} \right)^{0.5} = \left(\frac{150}{\pi \cdot 10} \right)^{0.5} = \underline{\underline{2.185m}}$$

The result shows that an appropriate air tank would need to be 10 meters long and would have a diameter of around 4.4 meters. These dimensions exceed the proportions of the whole turbine casing by far and from this position it seems that this constellation is rather impossible to accomplish.

This applies even more for two other reasons. Firstly, the tank needs to be attached at the very front of the turbine, where the turbine gets narrower for aqua dynamic reasons. Secondly, I have not taken into consideration the turbine's own weight (especially the two pumps weigh around 1100kg each) which will further increase the necessary buoyant force.

In conclusion, this approach is not the wisest possible way. The air volume in the turbine casing needs to be enormous to keep the turbine safe above the seabed.

4.1.3. Turbine base construction: method 2

4.1.3.1. Overall concept

Another more realistic yet more complicated method is to build a base on the seabed. The base also consists of a concrete bottom but a pole is mounted on it which stands vertically out of the base. On the top of the pole is the mounting of the rope which is connected to the turbine.

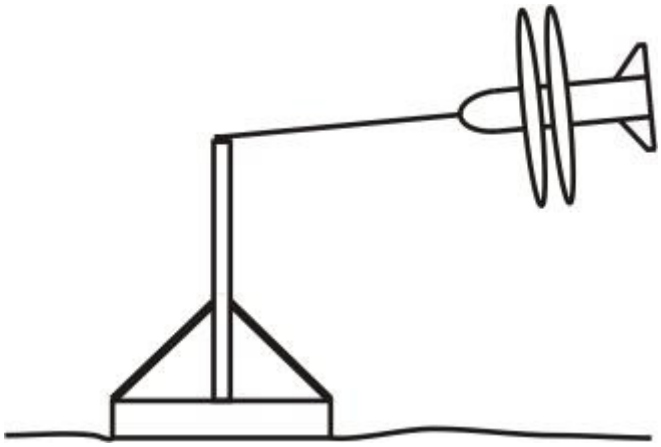

Sketch 4.3

The disadvantages of this system compared to the other one are the higher costs and complexity. However, having the turbine mounted on the pole means that the turbine's buoyancy can be close to zero and consequently the size problem of the air tank is not existent anymore.

Still, there is a need of a fair amount of buoyancy to let the turbine move like a pendulum from one side to the other. It is absolutely crucial that the turbine has sufficient lift to prevent it by any means from colliding with the pole.

On the other hand, for we want to keep the buoyancy as low as possible. Keeping the longitudinal axis of the turbine as parallel to the seabed as possible is equally important. So the mounting of the rope could be in the front centre of the turbine. Furthermore, this means that the pole length has to well over the radius of the turbine to not touch the seabed.

The bending force on the pole and the torque in the base caused by the turbine's tractive force will be considerably high. That is why I opt for a reinforcing of the pole. The main

pole should be strengthened by 4 other poles which are fitted in star formation in a 45° angle from the main pole to the base.

4.1.3.2. Air tank volume

The drag force of the turbine at cut-in speed is around 23 kN. So I choose a buoyant force of 1 kN to keep the turbine already at cut-in speed as horizontal as possible.

Turbine angle at cut-in speed: $\arctan\left(\frac{F_{B,2}}{F_{D,C}}\right) = \arctan\left(\frac{1}{22.665}\right) = \underline{\underline{2.526°}}$

Turbine angle at rated speed: $\arctan\left(\frac{F_{b,2}}{F_{D,R}}\right) = \arctan\left(\frac{1}{251.829}\right) = \underline{\underline{0.228°}}$

The angularity is so small that the losses of working surface will be negligible. The turbine will be 45° inclined at 0.16m/s.

The necessary air volume is around 0.1m³ and can be easily placed in the front of the turbine. In cylindrical shape the tank has a radius of 0.25 m and a length of 0.5 m.

4.1.3.3. Base dimensioning

At the critical point the force f_1 would be zero. As the radius of the rotor is 5.3 meters, I choose a pole length of 7 meters (8 - 10 m, if e.g. unknown seabed condition) to be safe above the sea bottom. I assume that the best geometry for the base would be a flat cylinder. F_1 and F_2 are the reaction forces on each end of the cylinder (2-dimensional front-perspective) resulting from the base weight. $F_1 + F_2 = F_{TB}$.

Rated drag force	$F_{D,R} = 251.829$ kN
Radius of base	$r_{TB} = 3$ m
Pole length	$l_m = 7$ m

$$F_{D,R} \cdot l_m = F_2 \cdot r_{TB} \quad \Rightarrow \quad F_2 = \frac{F_{D,R} \cdot l_m}{r_{TB}} = \frac{251.829 \cdot 7}{3} = \underline{\underline{587.601kN}}$$

This would mean that the weight force of the base has to be half of F_2.

$$F_{TB} = \frac{F_2}{2} = \frac{587.601}{2} = \underline{\underline{293.801kN}}$$

Considering a safety factor of 1.5,

$$m_{TB,sf} = 293.801 \cdot 1.5 = \underline{\underline{440.702kN}}$$

The under sea conditions lead to a lower density difference and increases the required concrete volume.

Concrete density $\rho_C = 2600 kg/m^3$

Base area $A_{TB} = r^2 \cdot \pi = 3^2 \cdot \pi = 28.274 m^2$

Cylinder height h_{TB}

$$h_{TB} = \frac{F_{TB,sf}}{g \cdot A_{TB} \cdot (\rho_C - \rho_W)} = \frac{440.702}{9.81 \cdot 28.274 \cdot (2600 - 1025)} = \underline{\underline{1.009m \approx 1m}}$$

So the overall height of the base including the pole is 8 meters.

Base volume $V_{TB} = A_{TB} \cdot h_{TB} = 28.274 \cdot 1.009 = \underline{\underline{28.529m^3}}$

Required base mass $m_{TB,total} = V_{TB} \cdot \rho_C = 28.529 \cdot 2600 = \underline{\underline{74175kg}}$

Equivalent (reduced) base mass under the water

$$m_{TB,total,R} = V_{TB} \cdot (\rho_C - \rho_w) = 28.529 \cdot (2600 - 1025) = \underline{\underline{45646kg}}$$

4.1.3.4. Dimensioning of main pole

For dimensioning the main pole, the point of interest is the junction between the main pole and the reinforcing poles where the biggest bending moment occurs.

Length from pole end to junction $l_{m1} = 4.1$ m

Rated drag force $F_{D,R} = 251.829$ kN

Bending moment at junction

$$M_{B,J} = F_{D,R} \cdot l_{m1} = 251.829 \cdot 4.1 = \underline{\underline{1032.499 kNm}}$$

The sea environment makes it necessary to consider a saltwater-resistant material. Steel - type 316 - is a commonly used marine grade stainless steel to avoid pitting corrosion.

Yield strength of steel 316 $\sigma_Y = 300$ N/mm^2

Factor of safety FoS = 1.5

Maximum allowable stress $\sigma_{max} = \frac{\sigma_Y}{FoS} = \frac{300}{1.5} = \underline{\underline{200 N/mm^2}}$

Chosen dimensions to obtain a wall thickness s_m of 30 mm:

Outer radius $r_{2m} = 260$ mm

Inner radius $r_{1m} = 230$ mm

Moment of inertia of pole (annulus) $I_m = \frac{1}{4} \cdot \pi \cdot (r_{2m}^4 - r_{1m}^4) = \underline{\underline{1.3912 \cdot 10^9 mm^4}}$

Check:

$$\sigma_B = \frac{M_{B,J}}{\frac{I_m}{r_{2m}}} = \frac{1032.499 \cdot 10^6}{\frac{1.3912 \cdot 10^9}{260}} = \underline{\underline{192.961 N/mm^2 \leq 200 N/mm^2}}$$

4.1.3.5. Dimensioning of supporting poles

The supporting poles are placed in 90° angle to each other. In the worst case, when the direction of the drag force of the turbine and the direction of the supporting pole to the main pole is the same, all the force goes on just two supporting poles plus the main pole. So the bending moment at the base is split up into three poles.

$$M_{B,B} = F_{D,R} \cdot l_m = 251.829 \cdot 7 = \underline{\underline{1762.803 kNm}}$$

$$M_{B,B,p} = \frac{M_{B,B}}{3} = \frac{1762.803}{3} = \underline{\underline{587.601 kNm}}$$

Chosen dimensions (wall thickness, s_s = 30 mm):

Outer radius r_{2s} = 200 mm

Inner radius r_{1s} = 170 mm

Moment of inertia of pole (annulus) $I_s = \frac{1}{4} \cdot \pi \cdot (r_{2s}^4 - r_{1s}^4) = \underline{\underline{6.007 \cdot 10^8 mm^4}}$

Check:

$$\sigma_B = \frac{M_{B,J}}{\frac{I_s}{r_{2s}}} = \frac{587.601 \cdot 10^6}{\frac{6.007 \cdot 10^8}{200}} = \underline{\underline{195.650 N/mm^2 \leq 200 N/mm^2}}$$

4.1.3.6.Rope dimensions

Actual rope length will also depend on the water depth respectively tidal range of the site. A rope length of around 10 meters is realistic. The safety factor for the rope should be at least 5 because it is a neuralgic part of the plant and ensuring service security is a predominating factor. I assume $F_{D,R} = F_{R,R}$ as the buoyant force F_B is negligible.

$$F_{D,R,sf} = F_{D,R} \cdot sf = 251.829 \cdot 5 = \underline{\underline{1259.145 kN}}$$

The company *Teufelberger* produces steel wire ropes for offshore applications. Their non-rotating wire rope *TK 16 Evolution* has a very high breaking load of 1369 kN at a diameter of 38 mm and an extended service life, which is lowers maintenance costs. Its high-torque stability helps the turbine to stay steady.

4.1.3.7. Considerable points

I have now calculated the basic dimensions of the unit which makes it possible to consider eventual effects. The poles, specifically the main pole, might produce some significant drag because of its circular shape, which could have finally an impact on the dimensioning of the concrete base. A low drag (wing) - shape would for sure be advantageous, anyhow, as the turbine moves freely, it is unrealistic that the water flow will always point at the low drag frontal area. If the angle between water stream and front end of pole is too big, it could be even disadvantageous not mentioning the lower mechanical stability of this shape.

So to get the Reynolds-number I need first to obtain the drag coefficient for the pole.

Dynamic viscosity of water $\eta_W = 1 * 10^{-3}$ kg/ms

Kinematic viscosity of water $\nu_W = \eta_W / \rho_W = 1 \cdot 10^{-3} / 1025 = 9.756 \cdot 10^{-7}\ m^2/s$

Main pole diameter $d_{2m} = 0.56$ m

$$\mathrm{Re} = \frac{V_R \cdot d_{2m}}{\upsilon_w} = \frac{2.5 \cdot 0.56}{9.756 \cdot 10^{-7}} = \underline{\underline{1.435 \cdot 10^6}} \quad \Rightarrow \quad \text{Turbulent}$$

Drag coefficient of pole (cylinder shape) $c_{D,m} = 0.6$

Frontal surface of pole $A_m = l_m \cdot d_{2m} = 7 \cdot 0.56 = 3.92 m^2$

Drag force at rated speed

$$F_{D,R,m} = \frac{1}{2} \cdot c_{D,m} \cdot \rho_W \cdot A_m \cdot V_R^{\ 2} = \frac{1}{2} \cdot 0.6 \cdot 1025 \cdot 3.92 \cdot 2.5^2 = \underline{\underline{7.534 kN}}$$

The drag force of the main pole is around 3% of the turbine's drag force. It would just slightly increase the necessary dimensions of the concrete base (increase of base height by 1 cm). Nevertheless, also the other poles and the base itself produce some drag – although those would not produce a big momentum on the base as they are close to the ground – and so it might be safer to increase the factor of safety from 1.5 to 2.

In addition, the turbine will never get into a state of complete horizontality because of the turbine's buoyancy, which means that the overall force on the base will be slightly higher (1kN). Its impact however is negligible (<0.5%).

On the other side, if the turbine is due to buoyancy not in a complete horizontal state at rated speed (which is likely), the drag will get smaller. Furthermore, the massive pole dimensions will add some extra weight to the base and so make it safer.

Mass:

Main pole: $m_m = 2.5$ tons

Supporting pole: $m_s = 1.1$ tons

So the extra mass coming from the poles makes around 7 tons (4*1.1 + 2.5), which does only little change to the overall base weight.

Additionally, there will be a loss of the turbine's working surface which is primarily caused by the main pole.

Turbine working area $A_{T,w} = 5.306^2 \cdot \pi = \underline{\underline{88.447 m^2}}$

Concerned frontal surface of main pole $A_{P,c} = 5.306 \cdot 0.56 = \underline{\underline{2.971 m^2}}$

3.4% of the turbine's working area are covered the main pole and perhaps an additional percent by the supporting poles. The actual resulting power losses are difficult to calculate and need to be tested. At this, the rope length, respectively the distance between pole and turbine plays the decisive role. The further away the turbine is placed from the pole, the lower are the power losses.

Concrete material: The use of seawater – resistant concrete, for example by adding Pozzolanic cement, fly ash or slag, is obligatory for a secure operation.

4.2. Generator Base - Platform

4.2.1. Platform size

The generator base, which is placed on the seabed, is the link between the turbine base and the platform. The main function is keeping the platform in a certain range on the surface. Another task is to insure that hydraulic cables run in an ordered way from the turbine base to the surface to prevent any conflict with the turbine.

The generator base has to withstand the force of the floating platform. This means that the size of the generator base depends on the drag force which the platform produces. Firstly, I need to have the size of the platform.

Considering that the generator on the platform is about 1 meter wide and 2 meters long and that the hydraulic pump with hoses is connected to the front of the generator, I would go for a platform dimension of 6 meters length and 4 meters width. This should give enough space to make an approach to each device from all sides possible. Additionally, I choose a platform height of 1 meter. A steel framework below can house for example cylindrical air tanks to accomplish buoyancy.

I estimate the weight of the platform around 2 tons and the devices 5 tons.

Platform volume $V_P = l_P \cdot w_P \cdot h_P = 6 \cdot 4 \cdot 1 = 24m^3$

Platform mass $m_P = 7000kg$

Mass displacement by platform $m_{P,D} = V_p \cdot \rho_W = 24 \cdot 1025 = 24600kg$

Immersion depth of platform $d_P = \frac{m_P}{m_{P,D}} = \frac{7000}{24600} = \underline{\underline{0.285m}}$

The mounting of the rope should be placed in the middle of the short side of the platform. This will help to keep the platform floating in a stable way, pointing at the water flow, compared to a centre attachment. Secondly, there is less drag on the narrower side of the platform.

4.2.2. Drag force on platform

The next step is to calculate the drag force of the platform, which I will do in a simplified way without considering the impact of waves and further geometrical details of the platform like the frontal area of the devices. The water current velocity can be higher on the surface because of the impact of wind and storm surges. I choose a maximum wind velocity of 50 m/s (*reference 2*).

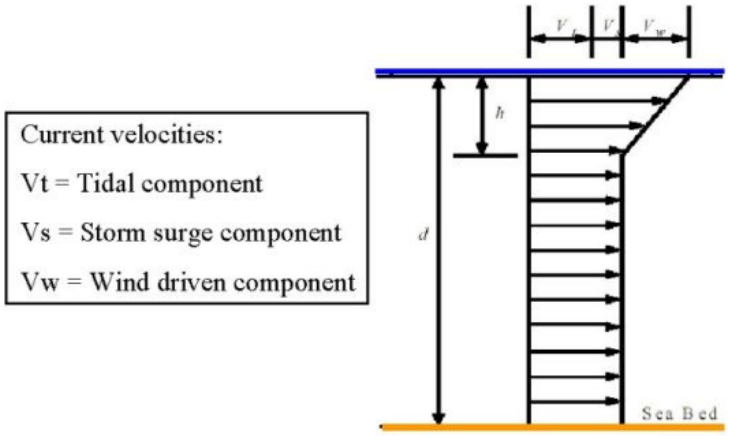

Picture 4.1

Maximum drag force on platform (immersed part)

Drag coefficient (plate shape)	$c_{D,P} = 1.1$
Max. Tidal current velocity on surface	$v_{max,\,s} = 4$ m/s
Immersed platform area (narrow side)	$A_{P,I} = 4 \cdot 0.285 = 1.14 m^2$

$$F_{D,P,I} = c_{D,P} \cdot 0.5 \cdot \rho_W \cdot A_{P,I} \cdot v_{\max,s}{}^2 = 1.1 \cdot 0.5 \cdot 1025 \cdot 1.14 \cdot 4^2 = \underline{\underline{10.283 kN}}$$

Maximum drag force on platform (protruding part)

Air density	$\rho_A = 1.25$ kg/m³
Max. Wind velocity	$v_{max,\,w} = 50$ m/s
Protruding platform area (narrow side)	$A_{P,P} = 4 \cdot (1 - 0.285) = 2.86 m^2$

$$F_{D,P,P} = c_{D,P} \cdot 0.5 \cdot \rho_A \cdot A_{P,P} \cdot v_{\max,w}{}^2 = 1.1 \cdot 0.5 \cdot 1.25 \cdot 2.86 \cdot 50^2 = \underline{\underline{4.916 kN}}$$

Total drag force on platform $F_{D,P} = 10.283 + 4.916 = \underline{\underline{15.199 kN}}$

4.2.3. Specifications of generator base

The necessary dimensions of the generator base are calculated similar to the turbine base. The highest force on the generator base occurs at neap tide. The rope is mounted centric on the generator base.

Radius of generator base $r_{GB} = 2{,}5$ m

Water depth at neap tide $l_{NT} = 40 - 6 = 34$ m

Angle of rope to vertical axis at neap tide $\alpha_{NT} = \cos^{-1}\left(\frac{34}{45}\right) = 40.926°$

$$F_{D,P} \cdot l_{NT} = F_{GB} \cdot r_{GB} \qquad =>$$

$$F_{GB} = \frac{F_{D,P} \cdot l_{NT}}{r_{GB}} = \frac{15.199 \cdot 34}{2.5} = \underline{\underline{206.706kN}}$$

Required base mass

$$m_{GB} = \frac{\frac{F_{GB}}{2}}{g} = \frac{\frac{206.706}{2}}{9.81m/s^2} = \underline{\underline{10536kg}}$$

FoS = 2,

$$m_{GB,sf} = 8627 \cdot 2 = \underline{\underline{21071kg}}$$

Generator base height h_{GB}

$$h_{GB} = \frac{m_{GB,sf}}{r_{GB}^2 \cdot \pi \cdot (\rho_C - \rho_W)} = \frac{21071}{2.5^2 \cdot \pi \cdot (2600 - 1025)} = \underline{\underline{0.681m}}$$

4.2.4. Platform – Base connection

Depending on the tidal range of the site the rope length has to be adjusted. A bigger tidal range means consequently that the platform has a larger cruising radius. Moreover, the larger the radius the bigger is the horizontal proportion of the force on the generator base. Still, the highest flow velocity and consequently force occurs between high and neap tide.

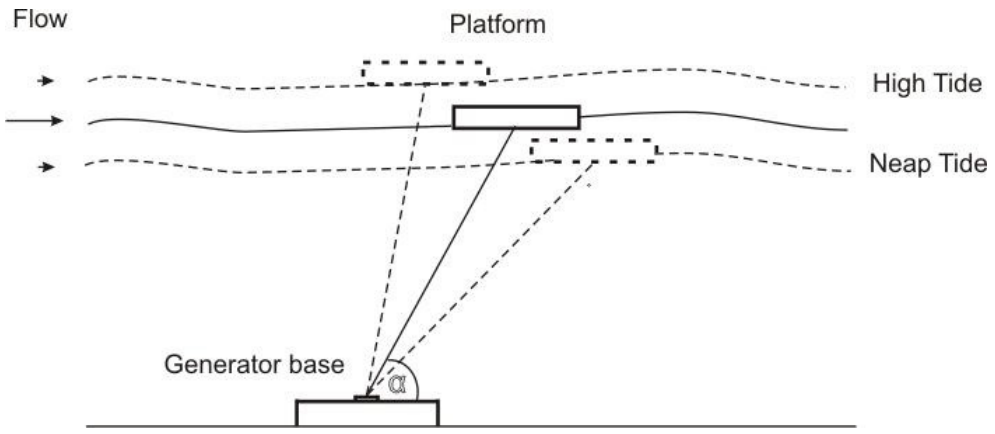

Sketch 4.4

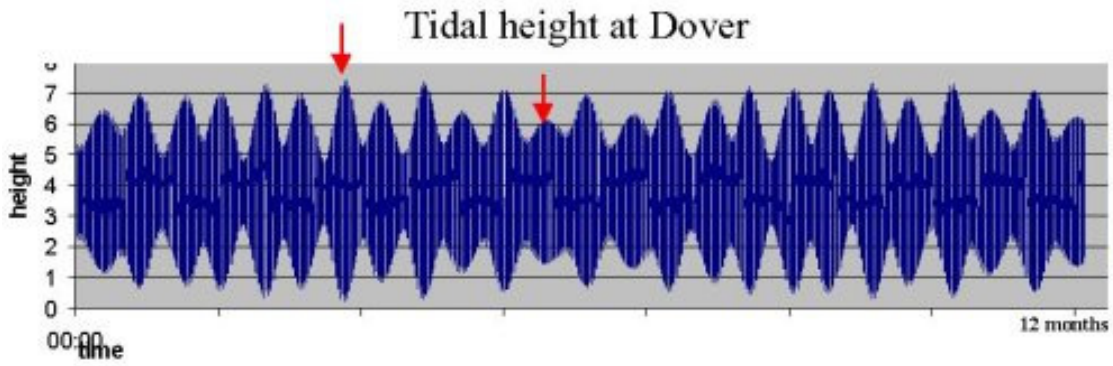

Picture 4.2

Chosen tidal range	6 m	(comparison: Bristol Channel 15 m).
Chosen water depth (high tide)	40 m	
Chosen rope length	45 m	

Rope should be a few meters longer than the maximum water level because of wave movement.

4.2.4.1. Force on rope

As shown in sketch 4.5 the highest speed is in the middle between maximum and minimum sea level. So the sea level at maximum speed is in our case

$$h_{sl,m} = 40 - \frac{6}{2} = \underline{\underline{37m}}$$

Having a rope length of 45 meters leads to an angle of

$$\alpha_m = \sin^{-1}\frac{37}{45} = \underline{\underline{55.308°}}$$

$$F_{R,R,GB} = F_{D,P} \cdot \cos(\alpha_m) = 15.199 \cdot \cos(55.308) = \underline{\underline{8.651kN}}$$

I round the value up to 10 kN. As I will describe later, we have to submerge the generator base in the set-up process. When we use this rope for the lowering operation, we have to dimension the steel wire in accordance with the highest possible force. So comparing the drag force of the platform (10 kN) with the mass of the base (21 tons), it is clear that the base will have a much bigger impact. The 21 tons of the base are around 210 kN.

As a result of neglecting the impact of waves in my calculations, a higher safety factor is preferable. The QS 816 VG from *Teufelberger* with a nominal diameter of 25 mm has a minimum breaking load of 846 kN and meets the safety demands satisfyingly (FoS = 8).

5. Testing: Turbine drag force

The strength of the steel wire between turbine and its base is immanent important to guarantee a secure operation. So after gaining the applied forces on a theoretical way, it is also necessary to test the actual drag of the turbine. As the University has access to a testing facility and to get fast and cheap results, a 35 cm long wooden model is built, which will be dragged through the water of the test tank simulating the real turbine. In contrast to the turbine axis, which can be easily created, constructing the blades is far more complex. We can, however, avoid this construction by mounting a metal wire mesh normal to the turbine axis on the model instead of the turbine blades and thereby simulate the blades. When we find a mesh which has approximately the same drag coefficient as the blades of the turbine, we achieve an enormous simplification of the model.

The measurement of the drag force will accomplished by using a strain gage, whereas the rope has to be divided in two parts and the strain gage will be placed in the middle.

5.1. Betz Theory

The *Betz*-theory (*reference 1*) delivers the theoretical background to calculate the drag coefficient of the mesh. The flow through the plane of rotation of the rotor is considered to be represented by a disc (Picture 5.1).

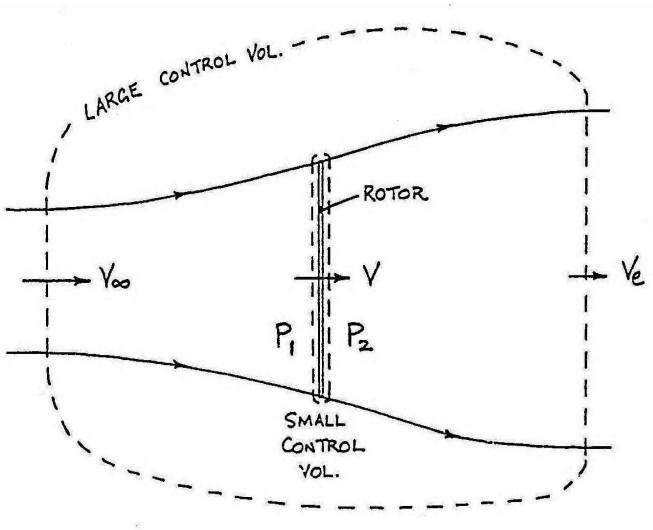

Picture 5.1

The relation between V and V_∞ can be defined by the variable a (shown in the equation below), the so-called *axial reduction factor*, which describes the deceleration of the wind caused by the rotor.

$$V = V_\infty (1 - a)$$

$$V_e = V_\infty (1 - 2a)$$

Extractable power by the rotor

$$P = \rho A V \frac{V_\infty^{\,2} - V_e^{\,2}}{2}$$

$$P = 2\rho A V_\infty^{\,2} (1 - a)^2 a$$

For maximum power: $\frac{dP}{da} = 0 \qquad (1 - 3a)(1 - a) = 0$

Max.: a = 1/3

Min.: a = 1

$$P_{max} = \frac{1}{2}\frac{8}{9}\rho A V_{\infty}^{3}$$

For maximum power output the value of C_D is 8/9.

5.2. Mesh test in duct

5.2.1. Calculating drag force of mesh

For substituting the rotor by a wire mesh, we need to find its flow resistance compared to a turbine. Thus we place different meshes into test duct and measure the wind speed differences at different crucial points to draw conclusions about their resistances.

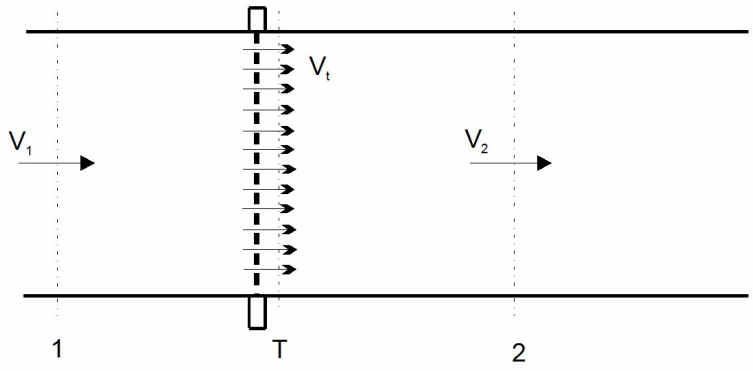

Sketch 5.1

At mesh level a large number of high-speed jets are produced with a velocity of V_t. After the mesh the flow slows down to V_2.

$$\frac{p_1}{\rho} + \frac{V_1}{2} = \frac{p_2}{\rho} + \frac{V_2^{\,2}}{2} + loss$$

$$loss = \frac{p_1 - p_2}{\rho} = \frac{(V_1 - V_2)^2}{2}$$

Continuity equation: $$A_t V_t = A_2 V_2$$

Now it is necessary to get A_t, therefore we need to define the *effective solidity* σ (which is not the actual solidity), so that $A_t = A_2(1-\sigma)$.

$$V_t = V_2(\frac{A_2}{A_t}) = \frac{V_2}{1-\sigma}$$

$$\frac{P_1 - P_2}{\rho} = \frac{(V_t - V_2)^2}{2}$$
$$= \frac{V_2^2}{2}\left[\frac{1}{1-\sigma} - 1\right]^2$$
$$= \frac{V_2^2}{2}\left[\frac{\sigma}{1-\sigma}\right]^2$$

$$\frac{P_1 - P_2}{\rho} = \frac{V_2^2}{2}K \qquad K = \left(\frac{\sigma}{1-\sigma}\right)^2$$

So K is defined as the energy loss coefficient in the duct. Next we want to compare K with the drag coefficient in the free flow system shown in sketch 5.1. When we assume that a is 1/3, then the velocity through the rotor V equals 2/3*V_∞.

$$F_D = \frac{8}{9}\frac{1}{2}\rho A V_\infty^2$$
$$= \frac{8}{9}\frac{1}{2}\rho A\left[\frac{3}{2}V\right]^2$$
$$= 2\frac{1}{2}\rho A V^2$$

So when we consider V rather than V_∞, the drag coefficient in this equation gets 2.

Force on mesh in duct (sketch 5.1)

$$F_D = (P_1 - P_2)A$$
$$= K\frac{V_2^2}{2}\rho A$$
$$= K\frac{1}{2}\rho A V_2^2$$

So we can say,

$$K \equiv C_D$$

In order to able to produce K = 2, it is preferable to know the solidity of a suitable mesh.

$$K = 2 = \left(\frac{\sigma}{1-\sigma} \right)^2$$

$$\frac{\sigma}{1-\sigma} = \sqrt{2} \qquad \sigma = \sqrt{2} - \sigma\sqrt{2} \qquad \sigma\left[1+\sqrt{2}\right] = \sqrt{2}$$

$$\sigma = \frac{\sqrt{2}}{1+\sqrt{2}} = \underline{\underline{0.586}}$$

So for getting proper test results of the model's drag force, a mesh is required, which has approximately a solidity of 0.5 and which is also stiff enough to not bend under stress.

5.2.2. Test of meshes in duct

I test 3 meshes which all have completely different design, structure and solidity. I attach each on the inlet of the duct (Picture 5.2). It contains an orifice plate and is populated alongside with an array of U-manometers.

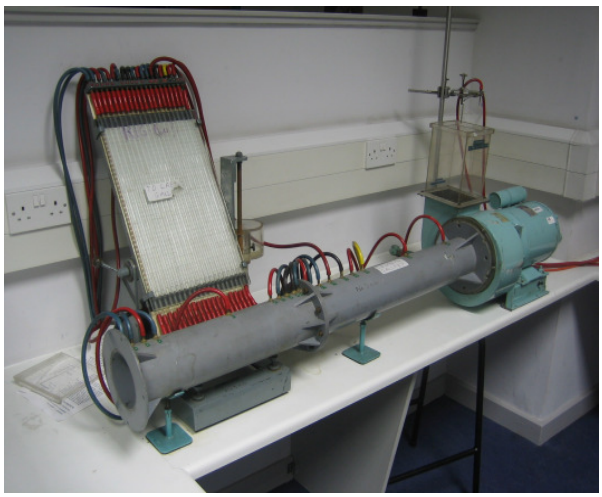

Picture 5.3

U-manometers:

h_2 - h_6……..placed before the orifice plate

h_{12} - h_{13}…...placed after the orifice plate

h_{20}…….....atmosphere

Area of tube outlet: A_O = 12.7 cm * 11.45 cm = 145.415 cm²

Atmospheric pressure: p_0 = 1.004 bar

Room temperature: T = 21 °C = 294.15 K

Air density: $\rho_A = \frac{p_0}{R_c T} = \frac{1.004 * 10^5}{287 * 294.15} = 1.189 kg / m^3$

5.2.2.1. Without mesh

The outlet of the duct behind a radial compressor has a rectangular shape and is split via a jig into 16 equal sections. First I need to find out the air volume flow through the duct. So I place a Pitot - static tube in the middle of each section and measure the height difference in the U-manometer.

1. Test series [cm]:

Sections	1	2	3	4	
1	8,6	5,8	5	5,6	
2	8	8	5,6	4,9	
3	10,6	7,9	5,9	5,5	
4	9,4	5,5	5,4	6,4	
Sum	36,6	27,2	21,9	22,4	108,1

Table 5.1

2. Test series [cm]:

Sections	1	2	3	4	
1	8,3	5,6	4,9	5,4	
2	8	7,7	5,6	4,8	
3	10,5	7,8	5,6	5,4	
4	9,2	5,3	5,3	6	
Sum	36	26,4	21,4	21,6	105,4

Table 5.2

Overall sum	213,5
average (213,5/32)	6,672

So the average height of all sections in two test series is 6.6719 cm. The U-manometer is placed in an angle of 6°, which means that the real height difference is factor 10 smaller (h = 0.667).

Then I measure the static pressures at the crucial points of the duct. The U-manometers are positioned of the test duct in an angle of 30° to the horizontal level, so the results have to be divided by 2.

	Measured height	Real height
h_{20}	4.9 cm	2.5 cm
h_6	8.2 cm	4.1 cm
h_{13}	28 cm	14.0 cm

Table 5.3

In order to proceed I need to get the fluid velocity. I derive the equation from the Bernoulli principle. I look on the pressure at point x in the U-tube.

ρ_m…… density of medium (water)

y……..height difference between Pitot-tube end and upper limit of fluid

Left side of duct: $$P_x = P_0 + \rho g y + \rho g h = P_1 + \frac{1}{2}\rho V_1^2 + \rho g y + \rho g h$$

Right side of duct: $$P_x = P_0 + \rho g y + \rho_m g h$$

So that $$\frac{1}{2}\rho V_1^2 + \rho g h = \rho_m g h$$

Flow velocity:

$$V_1 = \sqrt{2\left(\frac{\rho_m}{\rho} - 1\right) g h} = \sqrt{2\left(\frac{1000}{1.188} - 1\right) * 9.81 * \frac{0.667}{100}} = 10.421 m/s$$

Volume flow: $$Q = V_1 A_O = 10.421 * 145.415 * 10^{-4} = 0.151 m^3/s$$

Having the volume flow makes it possible to determine the effect the orifice plate has on the air flow through the duct.

Orifice flow coefficient: $K = \frac{Q}{\sqrt{h_{12} - h_6}} = \frac{0.151}{\sqrt{0.140 - 0.041}} = \underline{\underline{0.482}}$

After getting a value for K, I want to know if there is a measurable loss regarding the inlet of the pipe.

P_1…...pressure before orifice plate

K_L…..inlet loss coefficient

$$\frac{p_0}{\rho} = \frac{p_1}{\rho} + \frac{V_1^2}{2} + K_L \frac{V_1^2}{2}$$

Inlet diameter: $d_I = 10.3$ cm

Inlet area: $A_I = \frac{d^2}{4}\pi = \frac{10.3}{4}\pi = 83.232 cm^2$

Inlet speed: $V_1 = \frac{Q}{A_I} = \frac{0.151}{83.323 * 10^{-4}} = 18.122 m/s$

$P_0 = 1.003$ bar

$\rho_A = 1.188$ kg/m³

Get p1:

	measured height [cm]	real height [cm]
h_2	7,2	3,6
h_3	7,2	3,6
h_4	7,2	3,6
h_5	7,6	3,8
h_6	7,6	3,8
$h_{average}$	7,36	3,68
h_{20}	4	2
$h_{average}$ - h_{20}	3,36	1,68

Table 5.4

Considering again the angel of 30°, the height difference is 1.68 cm (3.36/2).

$$p_1 = p_0 - \rho g h = 1.003 * 10^5 - 1000 * 9.81 * 1.68 * 10^{-3} = 1.00135\, bar$$

$$K_L = \frac{2}{V_1^2}\frac{(p_0 - p_1)}{\rho} - 1 = \frac{2}{18.122^2}\frac{(1.003 - 1.00135) * 10^5}{1.188} - 1 = \underline{\underline{-0.154}}$$

K_L is very small and negative, which suggests inaccuracy of measurement. Therefore the inlet loss is considered negligible. => $K_L = 0$

Having now the value for K_L, I can check the values of V_1 and K retroactively.

$$V_1 = \sqrt{2\frac{p_0 - p_1}{\rho}} = \sqrt{2\frac{(1.003 - 1.00135) * 10^5}{1.188}} = 16.657 m/s$$

$$Q = V_1 A_I = 16.657 * 83.323 * 10^{-4} = 0.139 m^3/s$$

$$K = \frac{Q}{\sqrt{h_{12} - h_6}} = \frac{0.139}{\sqrt{0.140 - 0.041}} = \underline{\underline{0.442}} \neq 0.482$$

We can that the value of K differs depending on the way of calculation by about 10%. We will see later how this affects the overall results.

5.2.2.2. With mesh

After clarifying that there are no measurable losses in the pipe, I am able to finally place the first mesh on the inlet.

K_M……drag coefficient of mesh

$$\frac{p_0}{\rho} = \frac{p_1}{\rho} + \frac{V_1^2}{2} + K_M \frac{V_1^2}{2}$$

5.2.2.2.1. Mesh A - Square mesh with round threads

Solidity: σ = 0.592

	measured height [cm]	real height [cm]
h_2	10,20	5,10
h_3	10,00	5,00
h_4	10,00	5,00
h_5	10,00	5,00
h_6	10,20	5,10
$h_{average}$	10,08	5,04
h_{12}	24,80	12,40
h_{20}	4,80	2,40

Table 5.5

$$Q = K\sqrt{h_{12} - h_{ave}} = 0.482 \cdot \sqrt{0.124 - 0.0504} = 0.131 m^3/s$$

$$V_1 = \frac{Q}{A_I} = \frac{0.131}{83.323 * 10^{-4}} = 15.674 m/s$$

$$p_1 = p_0 - \rho g (h_{ave} - h_{20}) = 1.003 \cdot 10^5 - 1000 \cdot 9.81 \cdot (5.04 - 2.4) \cdot 10^{-2} = 1.0004\, bar$$

$$K_M = \frac{2 \cdot (p_0 - p_1)}{\rho V_1^2} - 1 = \frac{2 \cdot (1.003 - 1.0004) \cdot 10^5}{1.188 \cdot 15.674^2} - 1 = \underline{\underline{0.782}}$$

Calculating K_M using new corrected value of K = 0.442.

$$Q = K\sqrt{h_{12} - h_{ave}} = 0.442 \cdot \sqrt{0.124 - 0.0504} = 0.120 m^3/s$$

$$V_1 = \frac{Q}{A_I} = \frac{0.120}{83.323 * 10^{-4}} = 14.391 m/s$$

$$K_M = \frac{2 \cdot (p_0 - p_1)}{\rho V_1^2} - 1 = \frac{2 \cdot (1.003 - 1.0004) \cdot 10^5}{1.188 \cdot 14.391^2} - 1 = \underline{\underline{1.113}}$$

Second value of K_M is quite different from the first one possibly due to

- inaccurate measurements of the volume flow with Pitot-Static tube
- unclean U-manometers
- porous hoses between manometers and the test pipe

5.2.2.2.2. Mesh B - flat mesh with round holes

p = 1.025 bar

T = 21°C

ρ = 1.214 kg/m³

	Measured height [cm]	real height [cm]
h_2	12,00	6,00
h_3	11,60	5,80
h_4	11,60	5,80
h_5	11,40	5,70
h_6	11,60	5,80
$h_{average}$	11,64	5,82
h_{12}	20,80	10,40
h_{20}	4,00	2,00

Table 5.6

$$Q = K\sqrt{h_{12} - h_{ave}} = 0.482 \cdot \sqrt{0.104 - 0.0582} = 0.103 m^3/s$$

$$V_1 = \frac{Q}{A_I} = \frac{0.103}{83.323 * 10^{-4}} = 12.380 m/s$$

$$p_1 = p_0 - \rho g (h_{ave} - h_{20}) = 1.0025 \cdot 10^5 - 1000 \cdot 9.81 \cdot (5.82 - 2) \cdot 10^{-2} = 1.02125\, bar$$

$$K_M = \frac{2 \cdot (p_0 - p_1)}{\rho V_1^2} - 1 = \frac{2 \cdot (1.025 - 1.02125) \cdot 10^5}{1.214 \cdot 12.380^2} - 1 = \underline{\underline{3.031}}$$

Calculating K_M using K = 0.442.

$$Q = K\sqrt{h_{12} - h_{ave}} = 0.442 \cdot \sqrt{0.104 - 0.0582} = 0.095 m^3/s$$

$$V_1 = \frac{Q}{A_I} = \frac{0.095}{83.323 * 10^{-4}} = 11.353 m/s$$

$$K_M = \frac{2 \cdot (p_0 - p_1)}{\rho V_1^2} - 1 = \frac{2 \cdot (1.025 - 1.02125) \cdot 10^5}{1.214 \cdot 11.353^2} - 1 = \underline{\underline{3.794}}$$

5.2.2.2.3. Mesh C - square flat mesh

	Measured height [cm]	Real height [cm]
h_2	11,40	5,70
h_3	11,20	5,60
h_4	11,20	5,60
h_5	11,20	5,60
h_6	11,00	5,50
$h_{average}$	11,20	5,60
h_{12}	24,60	12,30
h_{20}	4,40	2,20

Table 5.7

$$Q = K\sqrt{h_{12} - h_{ave}} = 0.482 \cdot \sqrt{0.123 - 0.056} = 0.125 m^3/s$$

$$V_1 = \frac{Q}{A_I} = \frac{0.125}{83.323 * 10^{-4}} = 14.973 m/s$$

$$p_1 = p_0 - \rho g (h_{ave} - h_{20}) = 1.0025 \cdot 10^5 - 1000 \cdot 9.81 \cdot (5.6 - 2.2) \cdot 10^{-2} = 1.02166\, bar$$

$$K_M = \frac{2 \cdot (p_0 - p_1)}{\rho V_1^2} - 1 = \frac{2 \cdot (1.025 - 1.02166) \cdot 10^5}{1.214 \cdot 14.973^2} - 1 = \underline{\underline{1.454}}$$

Calculating K_M using K = 0.442

$$Q = K\sqrt{h_{12} - h_{ave}} = 0.442 \cdot \sqrt{0.123 - 0.056} = 0.114 m^3/s$$

$$V_1 = \frac{Q}{A_I} = \frac{0.114}{83.323 * 10^{-4}} = 13.731 m/s$$

$$K_M = \frac{2 \cdot (p_0 - p_1)}{\rho V_1^2} - 1 = \frac{2 \cdot (1.025 - 1.02125) \cdot 10^5}{1.214 \cdot 11.353^2} - 1 = \underline{\underline{1.919}}$$

5.2.3. Results

In conclusion, the two different values of K have a big impact on the value of the mesh drag coefficient K_M. Nevertheless, the drag coefficient differences between the meshes are quite big, which makes it still possible to distinguish them. Furthermore, we can state that not only the solidity but also shape of the mesh has a big, perhaps even bigger, effect on the K_M-value. Also mesh C is wider meshed than mesh A, it produces a much higher drag force, which is because it is made of flat wires rather than round ones.

	K_{M1}	K_{M2}
Mesh A	0.782	1.113
Mesh B	3.031	3.794
Mesh C	1.454	1.919

Table 5.8

As shown in the table above, mesh C is actually close to the target value of 2, though we can not be completely assured of how much these values vary from the real one. We decide to use mesh C and additionally mesh A for our testing, also because there are no more suitable meshes available. (Meshes A & B retested on the day after with only slight different values)

5.3. Test series in water tank

5.3.1. Pre-test procedure

After evaluating a suitable mesh, we can proceed with measuring the drag force applied on the actual model when towed through the water. As already mentioned the force on the rope will be measured by a strain gauge.

Beforehand, we need to find out the drag force of the model, so that we can choose a suitable strain gauge for this operation.

Mesh area $$A_M = \frac{\pi}{4} d_M{}^2 = \frac{\pi}{4} \cdot 0.3^2 = 0.071 m^3$$

Drag force at 1 m/s $$F_D = \frac{1}{2} C_D \rho_w A_M V^2 = \frac{1}{2} \cdot \frac{8}{9} \cdot 1000 \cdot 0.071 \cdot 1^2 = \underline{\underline{31.556 N}}$$

As we intend to accelerate the carriage up to around 1.5 m/s, we set 50 N as the rated load for the strain gauge, which is comparable to a speed of 1.26 m/s. The gauge will reproduce a voltage signal of 400 mV when 50 N are applied.

Picture 5.4 - Test tank with carriage

We fix the model on a nylon chord, which accommodates the strain gauge, and the other end of the chord is attached to a steel pole. The pole is clamped in a vertical position onto the carriage dipping one meter into water. Then the strain gage is connected to a

measurement amplifier over a quarter-bridge circuit. The rectified signal leads over a digital converter to a PC, where the data is recorded.

The plan is to perform some test series with different speeds and meshes, simulating the sinusoidal change of velocity of the tidal flow to collect data close to reality. After submerging the turbine model in the water, it hangs in a vertical position on the rope. Then we need to wait until the strain gauge gets adapted to the water temperature.

5.3.2. Test runs

At first, we try if everything in our system works by making some pre-test runs. We discover however that we have a lot of noise in our signal (voltage is hopping up and down). So we check everything again and find out that the sealing of the strain gauges is insufficient to secure the contacts from water. Still, we are equipped with two other strain gauges, which are also not well sealed, but one of them happen to have less noise and we agree to proceed.

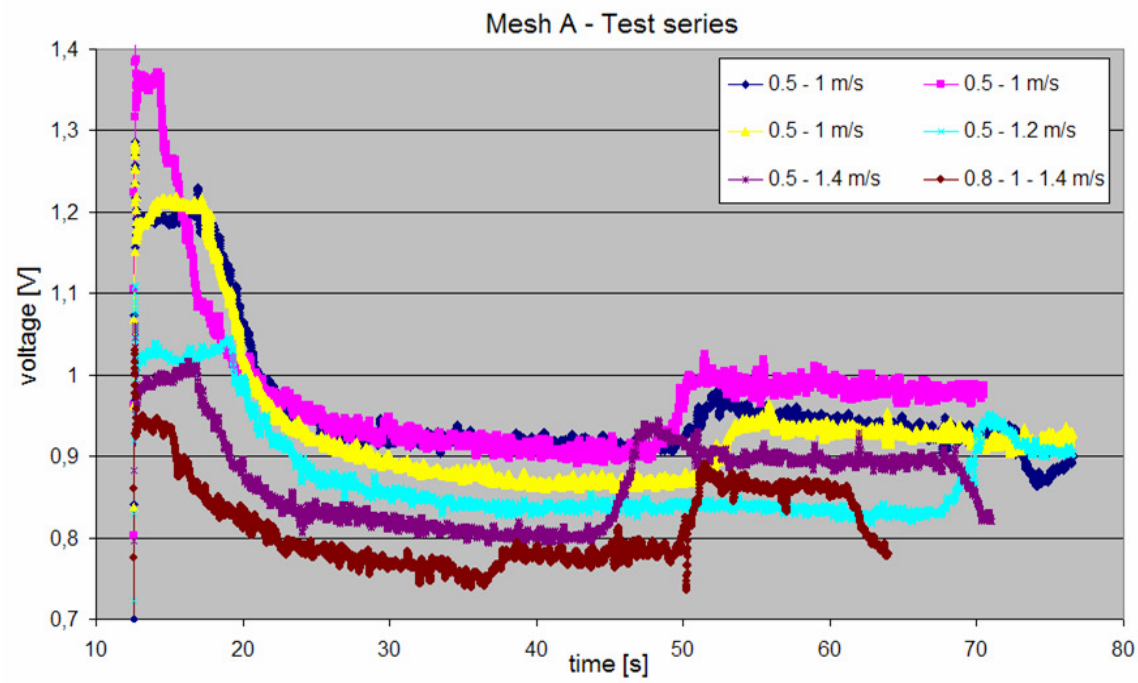

Diagram 5.1

Another challenge comes up in the wake of the sealing problem. As can be seen in diagram 5.1 – which shows 6 test series from day 1 - the voltage level raises until a certain level (at 12 sec.), when the carriage starts to accelerate. The voltage level remains constant

for a few seconds a then decreases though speed level stays the same. As the decrease is always an approximate 20% fraction of the original value, we can assume that is about a system immanent error.

This incident can be ascribed to different reasons:

- sudden backlash at the start of the acceleration
- decreasing drag of turbine (and mesh) when getting from vertical in horizontal position
- failure in strain gauge

In addition, we can state that the voltage level shows different values for each of the first 3 test runs although the speed (0.5 m/s) is always the same. Due to moisture in the strain gauge system the voltage level settles always down at another level. Consequently, we are not able to read off absolute values for the applied forces.

The only alternative to generate at least some information out of the test series is to change in each test run the speed at least one time. So we can get the voltage differences between the first and the second speed level (see diagram 5.1 at around 50 sec.). By repeating this test runs, like shown in the diagram above (e.g. 0.5 – 1 m/s), and also by varying the velocity-increases, we are able to compare these data series. So we can check in which way speed changes affect the drag force on the system.

As on test day 1 a lot of set up problems occur and we are only able to make a few test series until the end of the day, I mainly now concentrate on and analyse the data of the second test day. There we are able to collect far more data with a new set-up.

5.3.2.1. Testing drag force of mesh A – day 2

test number	Speed	voltage difference	
	m/s	Volts	Volts
test 1	0,5 – 1	0,066	------
test 2	0,6 - 1 - 1,4	0,051	no data*
test 3	0,6 - 1 - 1,4	0,040	0,070
test 4	0,5 – 1	0.073	------
test 5	0,4 - 0,8 - 1,2	0,037	0,068
test 6	0,6 - 1 - 1,4	0,046	0,065
test 7	0,5 – 1	0,054	------
test 8	0,4 - 0,8 - 1,2	0,025	0,074
test 9	0,6 - 1 - 1,4	0,045	0,075
test 10	0,5 - 1 - 1,5	0,047	0,095

Table 5.9

5.3.2.2. Testing drag force of mesh C – day 2

test number	Speed	voltage difference	
	m/s	Volts	Volts
test 1	0,5 – 1	0,026	------
test 2	0,5 – 1	0,030	------
test 3	0,6 - 1 - 1,4	0,026	0,040
test 4	0,6 - 1 - 1,4	0,028	0,038
test 5	0,5 - 1 - 1,5	0,029	0,052
test 6	0,5 – 1 - 1,5	0,032	0,050
test 7	0,5 – 1 - 1,5	0,031	0,050
test 8	0,8 – 1,2 - 1,6	0,037	0,049
test 9	0,8 – 1,2 - 1,6	0,038	0,062*

Table 5.10 * rope torn

5.3.3. First conclusions

The outcome of the testing is far from being optimal. As there are noise and voltage level changes after each test passage, the data quality might not be enough to draw distinct conclusions.

Firstly, we have to consider that the turbine is not placed horizontally, when dragged at low speed (e.g. 0.5 m/s). At around 1 m/s the turbine was nearly horizontal. This fact has probably quite an effect on the results as the mesh area is reduced on therefore drag force

will be even smaller than in theory. However, the increased frontal surface of the turbine body, due to inclined position, might have an inverse effect.
As I described in chapter 4, the prototype will be near to horizontal at any speed. So this issue regards mainly to the model, which does not have enough buoyancy.

Secondly, we use a nylon rope (fishing line), which should be capable of at least hundred kilograms (theoretically more), but still it tore on two occasions. In the second case the rope tore though I fixed the turbine with 2 ropes! One possibility is that the drag force on the turbine is higher than we originally assumed. An alternative explanation might be that a sudden peak of tractive force is exerted on the rope, when the carriage starts to accelerate. If the latter one is correct, then it will not cause problems in reality, because the tide accelerates slowly.

5.3.4. Comparing test results with calculations

We can compare the test results form the test tank with the values we gathered in the duct test and so prove the accuracy of these measurements. First, I average the voltage differences from tables 5.9 respectively 5.10 for each speed increase (see table 5.11). Then I take the ratio of mesh C and A, to see how stable their differences are (for No.1 and 7 not enough data). Besides No. 2 the values are quite stable and the average ratio counts exactly 1.8.

Starting from the strain gauge sensibility (50 N = 400mV = 1.26 m/s), I am able to calculate the voltage differences for each speed increase (see Diagram 5.2 and ‘original reference value’ in table 5.11). For comparing the reference values with the test data, the reference values have firstly to be divided by 4, because we halved both the gain and voltage level to cut down the noise level.

	average difference			Ratio	reference values		
		mesh C	mesh A	mesh C /mesh A	original	mesh C	mesh A
No.	m/s	Volts	Volts		Volts	Volts	Volts
1	0,4 - 0,8	0,031			0,120	0,030	0,016
2	0,5 - 1,0	0,056	0,030	1,856	0,187	0,047	0,025
3	0,6 - 1,0	0,044	0,027	1,617	0,160	0,040	0,022
4	0,8 - 1,2	0,071	0,038	1,868	0,200	0,050	0,027
5	1,0 - 1,4	0,070	0,039	1,795	0,250	0,063	0,034
6	1,0 - 1,5	0,095	0,051	1,863	0,315	0,079	0,042
7	1,2 - 1,6		0,049		0,280	0,070	0,038
ave.				1,800			

Table 5.11

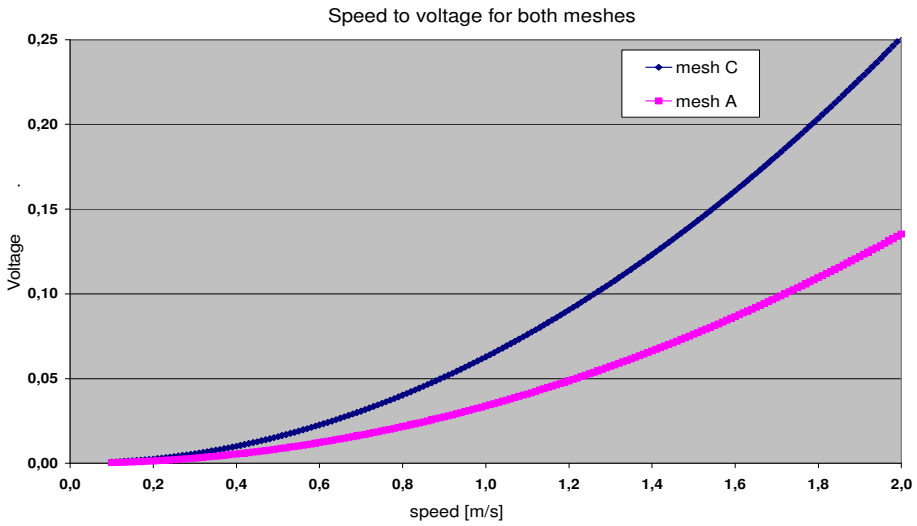

Diagram 5.2

After doing that I set the reference values of mesh C equal to the original reference. I can do that, when mesh C has a K-value of 2. That is nearly the case of the K_{M2}-value of mesh C (K_{M2} = 1.919, see table 5.8). I get the reference values for mesh A by calculating the ratio between both K_{M2} – values.

$$\frac{K_{M2}(meshC)}{K_{M2}(meshA)} = \frac{1.919}{1.113} = \underline{\underline{1.724}}$$

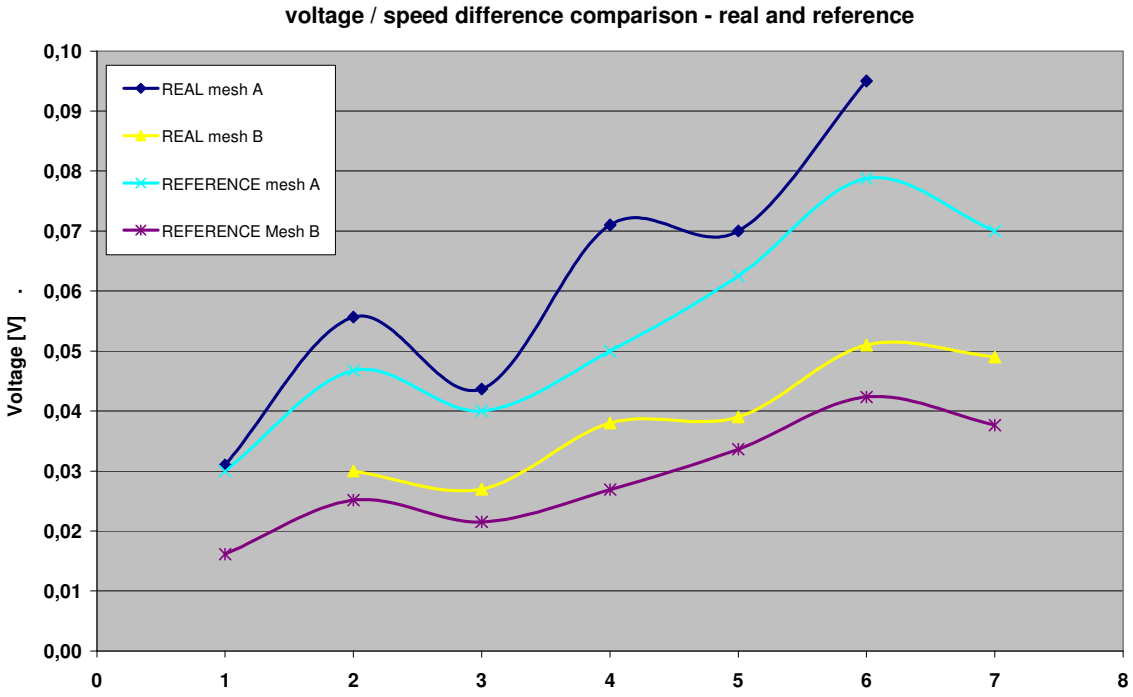

Diagram 5.3

When we now compare the reference ratio of 1.724 with the average ratio from the tank test (1.800), we can state that theory and experiment are matching surprisingly well.

Diagram 5.3 shows the voltage differences for the test series listed in table 5.11. Leaving testing point 4 for mesh A aside, real and reference values are coherent. Apparently, the values of the test tank are slightly higher than their theoretical counterparts. The undulating shape of the functions results from the varying speed - and consequently force - ranges (see table 5.11).

So due to extensive comparing, we can finally agree that the drag forces which the turbine actually produces in reality are close to our calculations. Nevertheless, absolute values are missing. The fact that the used rope tore twice during testing amplifies the demand for further testing in order to ensure operational security for future prototypes.

5.3.5. Further considerable aspects

	model weight (N)		resulting force F	drag force FD	F/FD	Angle [°]
	in air	in water	at 0.5 m/s			
mesh A	10,3	1	7,917	7,854	1,008	7,256
mesh B	12,3	2,5	8,242	7,854	1,049	17,657

Table 5.12

The model weight has small influence on the measurements. At low speed (0.5 m/s) the difference between the measured force F and the drag force F_D is 0.8% respectively 5%.

6. Implementation issues

Another complex part of the project is setting up the string of devices in an orderly way but also ensuring an easy access to all modules for maintenance and repair issues.

6.1. Maintenance

As it is always desirable to keep maintenance and service costs low, one of the initial conditions of the project, I mentioned it already earlier, is avoiding the involvement of diving personnel by all means. Having all devices of a plant attached together on one pier, like in the *seaflow* project (the turbine is liftable to the surface along a column) is a huge advantage. The hydraulic motor and the generator are situated on the platform, but the turbine, pumps and its base, however, are fully immersed and there is no direct mechanical connection to the surface. This fact makes it necessary to think about alternative solutions to get access to those units.

There are numerous approaches to solve this problem yet no one is overly satisfying. I see basically two different solutions. The first one is finding a mechanism to lift the turbine alone to the surface, whereas the second one is to lift turbine base and turbine altogether.

6.1.1. Solution method 1

Lifting only the turbine instead of the whole construction is seemingly a simpler task. The idea is to install an extendable rope between the turbine and the base so that the turbine can be heaved for service purposes. The rope runs from the turbine to the top of the main pole, continues inside the pole down to the bottom, then leaves the pole over a deflexion pulley and rolls up on a rope drum. The rope drum is controlled by a hydraulic motor which is placed besides. The winch is operated via a pump on the generator base and its hoses run in the same way as the power supplying hoses do (sketch 6.1).

For maintenance the hydraulic circuit of the rope drum - motor has to be unblocked and the hydraulic motor of the turbine has to be blocked. The turbine then rises to the surface because of its buoyancy and without actuating the motor. After inspection the motor starts to wind up the rope until the original position is reached.

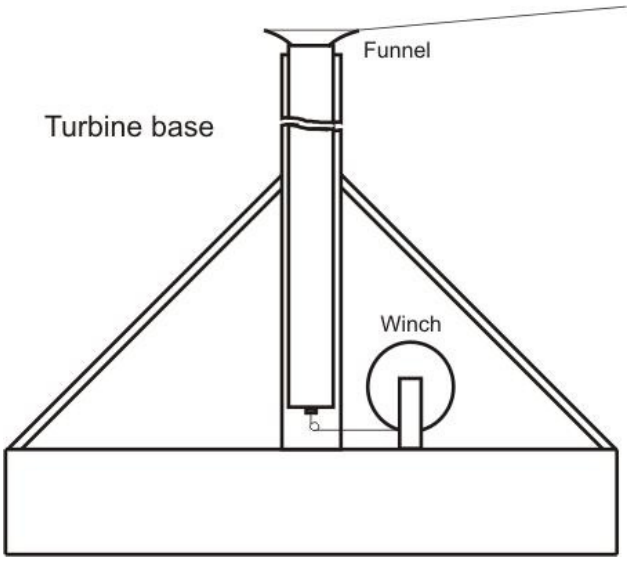

Sketch 6.1

The upper end of the main pole will need an adaptation to insure that the cable runs into the pole properly. I suggest designing the top of the pole funnel-shaped. The advantages of this construction are, firstly, to allow the cable respectively the turbine to move freely in the preferred direction. Secondly, building a round end on the inside of the pole deburrs the pole end and prevents the cable from buckling. Thirdly, the neck of the funnel works as a cable routeing and keeps the cable in the middle.

The force on the deflexion pulley and the rope drop will depend on the friction between rope and funnel. This will need further investigations. For preserving security the deflexion pulley needs to be dimensioned in such a way to withstand the rated drag force and the buoyant force (which is comparably small) of the turbine.

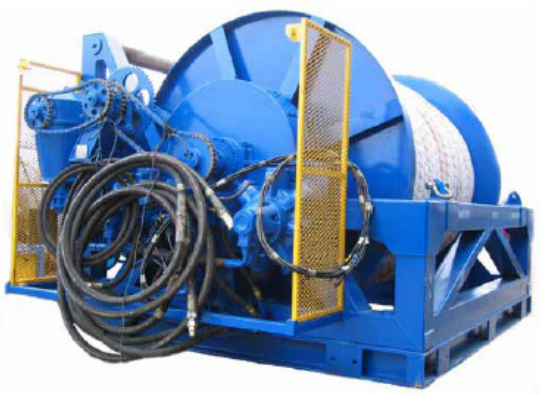

Pictures 6.1 & 6.2

The driving power of the winch can be relatively small as it just needs to be enough to cope with the turbine's buoyancy of 1kN, which is no problem for a small hydraulic winch. However, the turbine's rated drag force of 250 kN - equivalent to 25 tons - means that the winch is exposed to much higher forces during operational periods. The consequence is that only a winch with much larger with a high 'maximum brake holding' is be applicable.

Aberdeenshire-based manufacturer *Fisher Offshore* has hydraulic winches with deep water capability in production. Their maximum SWL (Safe Working Load) is 20 tons which is slightly below our demands, but customisation is possible.

The *Timberland Series 501* (shown right above) has a maximum brake holding of 80 tons which provides, on basis of the drag force, a security factor of more than 3. However, the exceeding dimensions and costs of this device make a realisation highly unlikely.

Other problematic issues

- The winch would need service from time to time and this would a fortiori demand diving personal.
- Stagnant machines in undersea – environment are at risk to become defective because of progressive fouling. A winch casing might be a proper protection.
- Probably the biggest issue is that the hoses between turbine and base would also need to be extendable in order to lift turbine. Although it would be possible to keep some extra meters of hoses at the generator base and to loosen them for maintenance purposes, it is rather unlikely to accomplish a smooth release and pull-back. It would need a sophisticated guiding rail to prevent the hoses from getting stuck.

6.1.2. Solution method 2

6.1.2.1. General

An alternative solution is lifting the complete system, including turbine and base. Lifting the whole rig has the advantage that all elements can be inspected and maintained, but also that the system turbine – base can remain unchanged without needing hose or rope

extensions. This means that much more power is required in order to lift also the heavier concrete base. Furthermore, the force has to be applied from an extern device.
When the turbine is stopped, it moves in a vertical position and thus its end is the closest spot to the surface. However, looking for an attachment at the end of the turbine to pull the rig to the surface is not recommendable as turbine and rope will need to be designed much more massive. Additionally, the turbine will stay under stress during maintenance, unless turbine and base are uncoupled. Therefore, the preferable solution is to attach the lifting rack to the base (sketch 6.2).

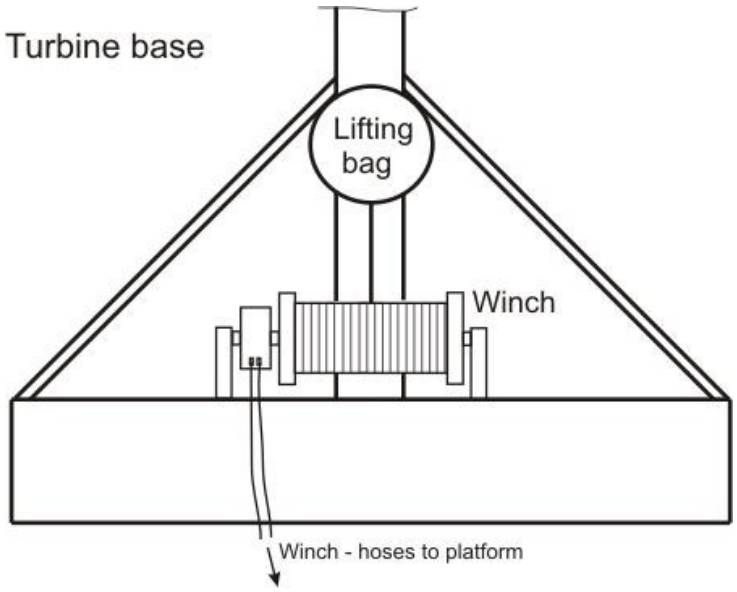

Sketch 6.2

The easiest way to get access to the turbine is placing a buoy on the surface, which is connected to the base over a heavy duty steel wire rope. However, there is a high possibility that the rope of the commuting turbine would get entangled with the buoy rope, why I rule out this option.

A more complicate but realistic method is to submerge the buoy respectively the air lifting bag and its cable. This can be accomplished by rolling the cable up a winch which is positioned right at the base. The force of the bag just needs to be enough to lift the rope. Once the bag has reached the surface, the end of the rope can be fixed to a ship-based crane and the base can be heaved.

For turbine inspections the base does not need to be lifted until the surface as only a few meters are required. The winch is driven by a hydraulic pump and is controlled from the platform.

6.1.2.2. Lifting bags

There exist various types of air lifting bags, but the main distinctive feature is whether the bag is open or closed. Whereas lifting bags with an open bottom, so-called parachute bags, are commonly used to heave goods from deep water, the closed form is mainly considered to give static support - meaning buoyancy - to devices like wrecks in shallow waters.

The opened version is more adequate for dynamic lifting operations. The bag is filled up at the bottom of the sea just enough to be able to lift the good, so that the buoyant force is slightly higher than the weight of the unit. It is important to not induce air excessively as it may lead to a loss of efficiency and it can be dangerous too.

Pictures 6.3 & 6.4 (*Left:* enclosed cylindrical design, *right:* open parachute design)

As hydrostatic pressure increases proportionally with water depth, the air volume in the lifting bag's air volume gets bigger the higher the bag rises in the water column. This means that the buoyancy of the lifting bag increases with its rise. Consequently, the bag accelerates which can lead to loss of buoyancy when the speed is too high and the bag gets deformed due to instability.

The risk of losing its buoyancy applies for both bag versions with however a further disadvantage for the open model which can lose also its air trough the bottom opening. In the worst case scenario the bag would sink back to the bottom of the sea.

The open system vents off the excess of air through the bottom opening and thus achieves a stable rising. Therefore, it is crucial to know the weight of the unit to calculate the necessary air volume and to choose the right bag size for the operation.

Another advantage of the parachute bag is that it, because of its design, always keeps an upright position compared to closed bag (picture shown below left). The enclosed cylindrical bag needs to be placed horizontally. It therefore needs two mounting points with two running cable wires, which have to measure the same length. If the lifting bag gets into a lopsided position, the air will migrate to places within the bag and so the lifting bag will loose its volume and consequently partly its buoyant force.

However, the parachute bag has also some disadvantages. First of all, high currents can harm the lifting operations as the bag might be displaced and brought into a position where it could dump air and thus lose its buoyancy. As a matter of fact, in our tidal power project we want to deploy our devices in places of high current velocity, which is a quite strong argument against open parachute bags. Furthermore, it is possible that the bag loses air when it has already reached the surface because of for example rough sea conditions.

The enclosed air bag vents off its excessive air through valves when it is ascending. In this case, if lifting velocity is too high, the vents will be overloaded and can not dump all waste air.

The problem with both versions is that they dump air and therefore need to be in- and deflated before and after each operation. The bags have to be fixed to the unit in an empty condition and then inflated. So the operation is based on the basic condition that diving personnel is securing, supervising and managing the load which in our case is not given.

On this account, neither the open nor the closed design is the proper device for this application. We need a bag which is capable of repetitive lifting and sinking operations

and most of all can be remotely controlled. So a more suitable model would be an enclosed bag without valves meaning a bag which keeps its air volume in any situation.

If a full enclosed bag is a realistic and also an affordable solution is arguable. Offshore companies which are producing lifting bags do not produce bags with this specification meaning that a custom-made product will be required.

When declining in water the pressure increases by approximately one bar every 10 meters. If we station the base at a depth of 45 meters, we will have a pressure difference of 4.5 bar compared to the atmospheric pressure. As a consequence, a full inflated enclosed bag at sea level will only have around 20% of its original volume at the bottom of the sea. So the bag will have lost a major part of its buoyancy. Furthermore, if this volume is still enough to heave the cable, the bag will rapidly increase its velocity while ascending which may lead to dangerous situations.

A considerable method is lifting the pressure of the bag at sea level from 1 to 5.5 bar in order to prevent the bag from diminishing in submerged condition. For this alternative solution the design of the lifting bag has to be adapted because material and structure is exposed to higher forces, which increases complexity and costs.

Reviewing all aspects, I would suggest the use of a *hard shell bag* is the best alternative**,** comparable to a buoy, which does not contract or expand at all. When taking a hard-shell air tank water depth becomes irrelevant as volume and pressure in the tank will not change and so its buoyancy remains constant over the water column. Realisation, feasibility, costs require further investigations.

6.1.2.3. Rope size

The actual cable strength depends on the mass of the base. The mass of the base is around 45 tons when submerged (74 tons in air) and the steel pole array adds another 7 tons. I neglect the near zero buoyancy of the turbine and so the overall weight is around 52 tons which concludes to approximately 510 kN. So considering the factor of safety is 5 the rope needs to endure at least 2550 kN.

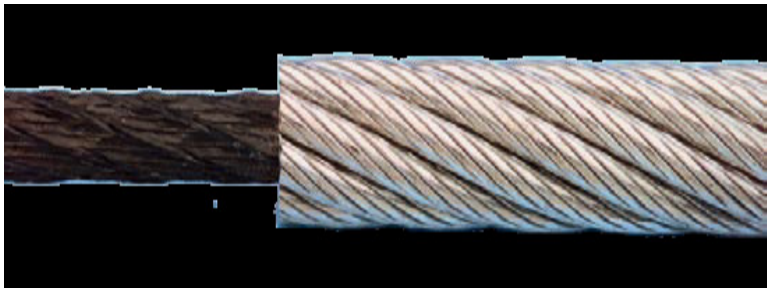

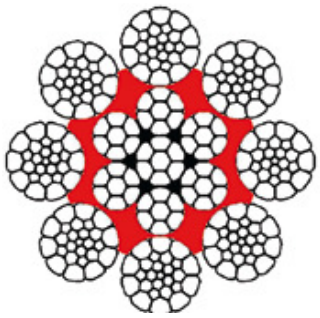

Pictures 6.5 & 6.6

The QS 816 V non rotation-resistant steel rope wire from Teufelberger can withstand loads up to more than 2000 kN. So by taking the thickest cable available, which measures 48 mm, a FoS of 4 would be possible, which is not sufficient. However, for higher demands custom products are still producible.

Cable type:	QS 816 V
Nominal thickness:	48mm
Minimum breaking load:	2046 kN (for medium quality: 1960 N/mm²)
Weight:	10.78 kg/m

6.1.2.4.Air bag size

Mass of cable (45m): $m_{TB,c} = m_c \cdot l_c = 10.78 \cdot 45 = 485\,kg$

Cable volume:

$$V_{TB,c} = \left(\frac{d_c}{2}\right)^2 \cdot \pi \cdot l_c = \left(\frac{0.042}{2}\right)^2 \cdot \pi \cdot 45 = 6.235 \cdot 10^{-2}\,m^3$$

Displaced water mass: $m_{D,c} = V_{TB,c} \cdot \rho_W = 6.235 \cdot 10^{-2} \cdot 1025 = 63.904kg$

Mass of cable in water: $m_{TB,c,w} = 485 - 64 = \underline{\underline{421\,kg}}$

Necessary air bag volume $V_{AB} = \frac{m_{TB,c,W}}{\rho_W} = \frac{421}{1025} = \underline{\underline{0.411m^3}}$

Considering a spherical air bag,

Air bag diameter $d_{AB} = \sqrt[3]{\frac{6 \cdot V_{AB}}{\pi}} = \sqrt[3]{\frac{6 \cdot 0.411}{\pi}} = \underline{\underline{0.922m}}$

So an air bag size of 0.92 m diameter would be enough to heave the rope wire to the surface. Due to the fact that the rope is furled on the winch in first place, there is less buoyancy required at the start of the lifting process. The more the wire is uncoiled, the more the buoyancy surplus gets reduced. By this rationality the air bag accelerates until a certain speed and then slows down because of increasing cable weight.

Additionally, there might be some friction losses for example in the winch, which will decrease the lifting force of the air tank. Omitting further investigations, I would recommend installing an air tank with a diameter of 1 meter, which would enhance buoyancy by 28%, to insure a successful lifting operation.

Another considerable point is to have the whole lifting progress controlled by the winch pump. In contrast to just open the pump valve and let the air bag heave the wire uncontrolled, the pump can eliminate speed fluctuations, prevent braking or speeding and provide a steady lift. The controlling of the lift can be done on the platform.

6.1.2.5. Disadvantages of method 2

- The buoy size can be small, because it only needs to heave the wire. So the winch drive does not need to be powerful as the buoyancy of the bag is just around 4kN (cable mass = 421kg). Nevertheless, the winch construct still needs to be dimensioned massively as it has to withstand all the weight force of the base. On comparison to method 1, no drag force is applied on the winch during operation, but the weight of the base in case of maintenance. So costs for the winch will be as high as in method 1. In my opinion, method 2 is still preferable, because there is long-term loading on the lifting unit and the method is less complex.

- The installation of a small hydraulic pump is still necessary in this approach. Consequently, there exists a certain potential that the pump fails and that a maintenance operation is not accomplishable. However, the buoyancy of the air tank should be sufficient that an unlocking of the hydraulic circuit lift the cable. By that way, the turbine unit is still salvageable and the pump can be repaired.

- In advance some extra meters of hoses need to be deployed between the turbine and the generator base on the bottom of the sea, because distance will increase between both bases when lifted. Nature of sea bed might be problematic.

- Another crucial point is to carefully measure the lifting process avoiding any kind horizontal deviation and place the base at the same spot after maintenance.

- Costs of lifting the base will possibly be higher due to increased demand for ship quality. The salvage method requires an installed crane onboard the ship, which is capable of heaving the unit.

- Base will tilt when lifted because of the offset mounting of the winch on the base.

- The winch also needs maintenance and cleaning might be necessary because of fouling.

6.1.3. Other approaches

- One possibility could be to place a buoy on the surface offset to the turbine base (see sketch 6.3). This buoy would be connected to turbine base over a strong steel cable wire. In order to avoid interacting between the wire and the commuting turbine, the cable has to run down vertically from buoy to the sea bed and then along the bottom to the turbine base. Thus another small base, call it cable base, needs to be set up exactly where the wire hits the ground, which acts as a corner support. The generator base could be used for this proposal, though it might be too heavy and operation would get too complex (too much things are fitted to the generator base).

  In case of maintenance a lifting of the cable would first heave the cable base but then would give access the turbine base.

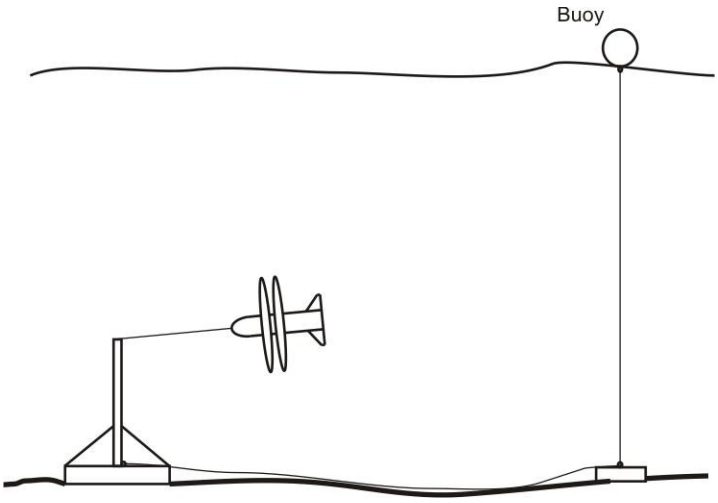

Sketch 6.3

- Another way might be to salvage the turbine via a magnet mounted on a ship-crane. Feasibility would need further investigation.

6.2. Set up

This chapter deals with the way of the whole plant is immersed and installed. First condition is having a ship placed at the disposal which is able to carry and handle the plant.

At site the first unit to be placed is the base of the generator. Most important is having all necessary hoses already attached to the base before immersing starts. For lowering the base we use the cable which will be connecting generator base and platform. Once the base has reached the bottom of the sea, one end of the wire ropes and the hoses will be mounted to the platform respectively to the hydraulic motor and the other ones are kept at the ship.

The next step is to navigate the ship to the place where the generator base will be immersed while starting to roll out the hoses along the seabed. At the spot, controlling and keeping a safe distance to the generator platform/base is the first objective. For this reason the hoses could be marked with length information. Secondly, turbine/base unit has to be fully assembled.

Assuming method 2 as the preferred solution, the turbine can be placed onto the water surface at first instance. Its buoyancy will prevent it from sinking. Then wire of the winch of the turbine base has to be connected with steel wire crane and the sinking process can get started. When immersion operation is completed the lifting buoy has to be mounted on end of the winch rope. Afterwards, the air tank can be submerged by activating the winch pump from the generator platform.

A crucial point for successful implementation is locking the turbine blades, before they are immersed as they would immediately start to turn in the water, if there was sufficient current. Thus the pressure in the hydraulic circuit must be established at the very beginning of the operation..

Distance between platform and turbine base depends mainly on the rope length between turbine and its base. Platform and turbine will both go with flow, so the distance between them will not alter largely.
Another concern regards the laying of the undersea cable which connects the generator with the grid. One possibility is to use the generator base also as mounting point for the grid cable, in other words to lead the cable from the generator down to the base and further on along the seabed to the shore. So also the power cable has to be installed to the generator base before submerged in the set-up process.

When connected to the grid the generator can be fully stressed by the voltage to ensure the blocking of the hydraulic system for set-up and maintenance purposes. Undersea cables have to be buried to avoid damages, which can be done by using high pressure water jets thus omitting extensive digging operations. This operation should be done before the actual set-up to ensure the string order of the whole operation.

7. Configuration perspectives

Overlooking the concept of the power plant, the spatial separation of turbine and generator offers us certain alternatives. From an economic perspective it makes sense to consider further configurations with the similar specifications to increase cost efficiency.

For example, we could use the generator platform and its base as a central spot and plant a reasonable number of turbines around it. So, all turbines would be connected to one centre-placed generator. Also a row-formation could be feasible depending on site.

The specifications of the generator would of course need adjustment. If we gathered 6 turbines of P_{rated} = 300 kW in star formation, hydraulic motor and generator would need adjustment.
At this dimension the advantages of a synchronous generator might outweigh the squirrel cage generator. A Synchronous generator is yet more expensive than an induction one, because it additionally requires an inverter. However it is also more reliable and efficient, which gains importance in this case where a downfall of one generator will lead to a power loss of 6 turbines.
However, leading the whole volume flow coming from the turbine-pumps in one hydraulic motor would need a massive custom construction. In order to avoid that, an array of smaller motors could be linked parallel to each other and led into the generator instead.

Given the amount of devices installed on this central platform - several motors, generator and inverter – designing a massive concrete platform will be preferable because of its easier accessibility and the increased security respectively reliability of the system.

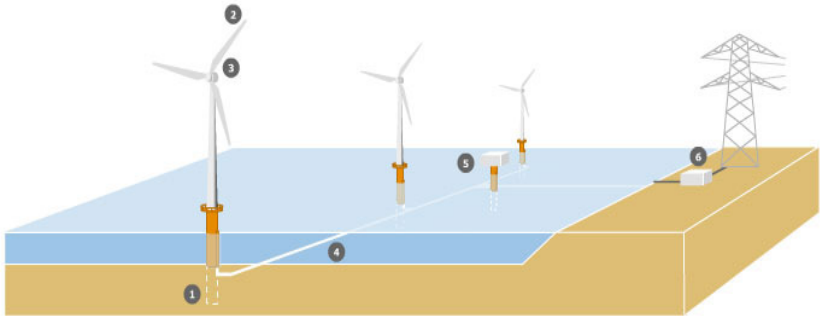

Picture 7.1

Sketch 7.1 shows an offshore wind farm with a quite similar approach to the one described above. The electric current coming from the turbines is demodulated and sent to mainland.

The idea of an array of turbines connected to a single generator can be further developed by regarding this plant as a remote station of an even bigger line-up. Like turbines are gathered in star formation around a generator base, generators can be linked over power cables between each other. One advantage is be that only one expensive shore-connecting power cable for the whole tidal turbine farm will be required. At the cable-linking point a converter along with a transformer could be installed to establish a high voltage direct current system (HVDC) as it leads less reactive losses. However, this option suits mainly tidal farms with long distances to the mainland and high power output.

8. Conclusion

On the overall, my view on the feasibility of installing a hydraulic power connection between turbine and generator is ambivalent. It is apparent that in the end it comes down to balance advantages and disadvantages. However, the most important factor besides the realisation potential are the overall costs.

Perhaps one of the most interesting characteristics is the possibility to connect more than one turbine to the generator (like it is shown in the previous chapter). As generators are one of the most expensive devices of a power plant, synergies can provide significant retrenchments. This means that for achieving a cost efficient solution, the power plant should have a minimum size respectively power output. This kind of configuration makes no sense for small-scale systems. However, if a failure occurs in the generator system, the whole array of turbines has to be turned down. Regardless of the configuration, omitting a massive concrete structure like in other prototype solutions will also save some money.

Another advantage is that the two coaxial, counter-rotating rotors produce zero torque and thus also no swirl. First, we save material and space but also increase efficiency compared to other single rotor solutions by installing two turbines together. Secondly, as the turbine can move freely in the water, we do not need to deploy a direction adjustment system.

Compared to other prototypes, the generator is situated on the water surface, which makes it easy to access in case of repair and puts it less at risk of failure.

On the other side, there are also some arguments to find which speak against a hydraulic drive-train. As separating generator and turbine has advantages, it also leads to the necessity of constructing, installing and maintaining two different – in our case – bases, whereas other technical solutions have *all in one*.

Furthermore, it is not without risk of operating a 300 kW (later on maybe even several MW) - turbine placed in the water hanging on a steel wire. A broken free turbine could cause substantial damage. It must be totally ensured that the cable is absolutely sufficient for this task. One option could be attaching a second cable which works as emergency wire.

Another problem is the maintenance intensive hydraulic circuit. Oil and oil filter of the chosen devices (Bosch, Hägglunds) have to be exchanged relatively often and so operational costs could be higher than with a conventional mechanical drive train. Moreover, the more devices are involved the higher the overall price, but also the higher the probability that one item fails.

As I described in chapter 6, getting access to the turbine itself is also a critical point. From my point of view, the described solutions are quite far from ideal. Once the turbine is submerged, it needs a relatively complex mechanism to make a remote controlled lifting possible. At this stage, I would not rule out that divers could do the job better and cheaper.

The hoses will also play an important role in deciding the feasibility of a hydraulic drive train. The bigger the turbine power will get, the exponentially bigger the hoses have to be built. At a certain level of volume flow, it is not enough to increase the flow speed as the stream will become turbulent. By increasing the diameter of the hoses, the construction belt will need to get exponentially thicker (and more expensive). The same happens when lifting the pressure in the hose. As a consequence, realising bigger power plants, e.g. 1 MW, will request especially constructed, very expensive hoses as also standard hoses are not available at this size.

If the decision is taken to build a concrete pier for the generator, the cost advantages, which were saved in comparison to other prototypes, would be extinguished.

Nevertheless, if marine current turbines will get more popular and their technique more advanced, companies will construct parts which are adapted exactly to the requirements. So also prices for a hydraulic drive train might fall.

The potential of this method lays in my opinion in the connection of a number of turbines to one generator. By doing so, all the costs of the generator base - including generator, hydraulic pump and concrete base – could be cut dramatically. When we install smaller turbines, we are able to use smaller and therefore cheaper hoses. Still, the overall output can be sufficiently big depending on the turbine-array size.

A Graphical excerpt

Diploma Project

Feasibility study of a hydraulically operated marine current power plant

Sascha Polak

Objective

- Limit CO_2 emissions
- Seeking alternatives to existing power generation methods (nuclear, oil, gas) which are carbon-neutral
- Consequence: Utilisation of natural resources
- Investing in renewable energy systems

Scottish natural resources

mainly

- Wind (on- and offshore)
- Water (river, storage, wave, tide)

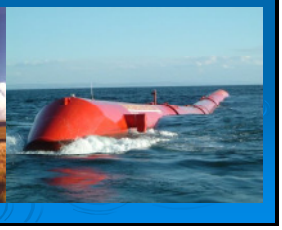

Tidal energy

Two different approaches

Barrage system

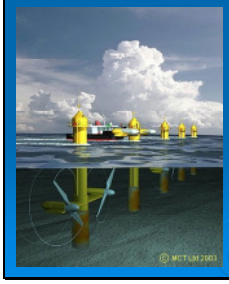

Marine current turbines

Marine Current Turbines

Pros

- Invisible
- Tidal cycle is fully predictable
- Variable scale
- Extendable → Tidal turbine farms
- Small impact on environment compared to *barrage system*
- More location options in contrast to *barrage system*

Cons

- Under water – access problem
- Offshore

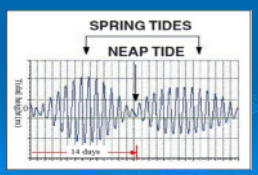

Project of the Strathclyde University

- Two counter-rotating rotors attached on one shaft

1st prototype 0.82m

2nd prototype 3m

Power transmission: Rotor - Generator
Two solutions

Mechanical
- Turbine-Generator unit
- Stable system
- Established technology
- Low maintenance

Hydraulic
- More configuration options
- No gearbox
- Self-aligning ability due to double-rotor system
- No concrete platform required

Hydraulic drive-train
Initial conditions

- Free-wheeling and floating turbine fixed to the seabed
- Generator afloat
- 300 kW rated power output

My Thesis

- Finding appropriate devices which fit to the specifications of the turbine and to the sea environment
- Providing a design concept of the power plant
- Considering maintenance, set-up and configuration issues
- Testing drag force of a turbine model

Initial design approach

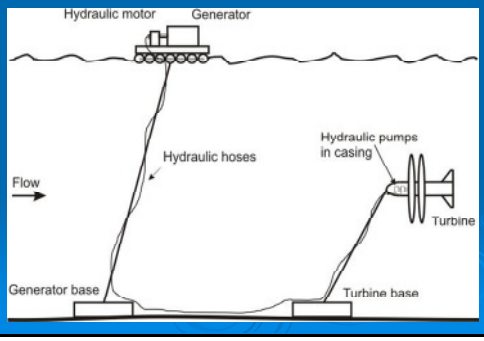

Drive - train

devices

Pump

- Turbine unfolds its power at low revolutionary speed (~16rpm at rated speed) in contrast to most pumps → *Hägglunds* pumps are suitable
- Necessity of two pumps
- Both pumps need to be located in front of the two rotors, because of hose-laying
- Offshore-capability

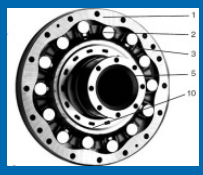

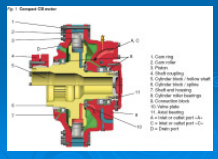

Hägglunds CB 540 – cam ring pump

Hydraulic motor

- By taking an hydraulic motor with a variable displacement, we can transmit the power directly to the generator without using a gearbox

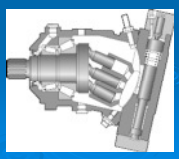

Bosch-Rexroth A6VM – axial piston motor

Generator

- For a rated power output of 300kW an *induction generator* is the best solution:
- Simple
- Cheap
- Reliable

Siemens - Offshore Wind Induction generator

Hoses

- Very high rated pressure (221 bar) requires an extremely reinforced hose (6 steel spirals)
- Very expensive (85 €/m) - overall: ~ 400m

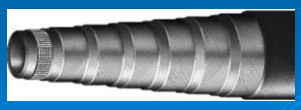

Diamondspir hose - Manuli-Hydraulics

Power plant design

Turbine base construction

Version 1

- Fitting an air tank in the front of the casing for required buoyancy
- A steel wire runs from the seabed to the nose of the turbine
- Off-centre attachment to keep turbine horizontal

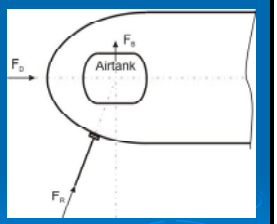

Turbine base construction

Version 1

- Simple
- Problem: Drag force varies highly depending on flow speed
- So *angle α* (Cable to perpendicular) varies
- Consequently, turbine is nearly never horizontal
- Air tank needs to be extremely big to minimize deflection
- Power loss due to deflection

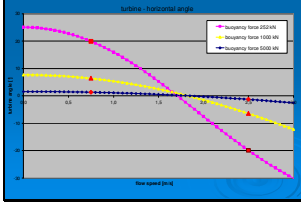

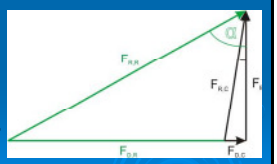

Turbine base construction
Version 2

- A better solution is mounting the steel wire on a turbine base
- The turbine just needs small buoyancy to change direction (swing)
- Turbine is horizontal most of the time
- More complex (expensive)

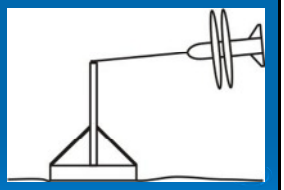

Platform – Generator base

- Platform can be floating or fixed (like oil platform)
- A fixed platform has the advantage of better accessibility, is yet more expensive

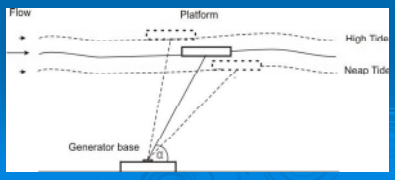

Drag force test

Drag force test (1)

- From *Betz' law*, we have the theoretical maximum of the drag coefficient of the rotor
- Verify value by testing a model in a tank
- For simplification, the rotors are substituted by a mesh
- Find a mesh with a suitable drag coefficient

Drag force test: Duct (2)

- Test the drag coefficient of 3 different meshes in a duct
- Select the one with closest drag coefficient value

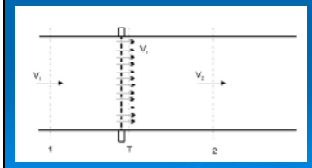

Drag force test: Test Tank (3)

- Testing drag force of model in a test tank at different speeds
- Analysing signal coming from a strain gauge, which is attached in the middle of two ropes

Drag force test: Test Tank (4)

- Problem: strong noise in the signal which made it impossible to receive absolute values

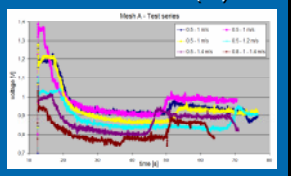

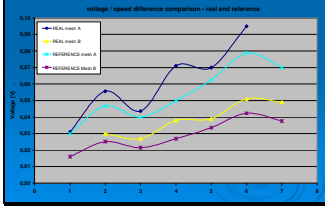

- Take relative values: measure and analyse speed differences
- Result: reference and real values are comparable

Implementation issues

Maintenance

- Problem: Inaccessibility of turbine once it is submerged
- Worked out 2 possible solutions

Maintenance: method 1

- Extendable pole
- Operated over a hydraulically driven winch
- Controlled by platform

- Complicate, expensive construction
- Assure the movability of the inner pole

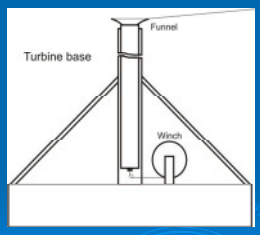

Maintenance: method 2

- Lifting bag
- Operated over winch
- Controlled by Platform

- Less complex
- Need to heave the whole base

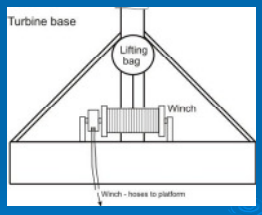

Configuration perspectives

- Usage of one generator for a league of turbines will cut down costs dramatically
- Problem: If generator is broken, the whole power plant farm is affected

Problematic issues

- Oil service – short intervals - expensive
- Hoses - expensive
- Security – ensure safety of turbine (rope)
- Reliability – under water (frail)
- No cohesive construction (complex)

B Bibliography

1. Betz, A. (1966) *Introduction to the Theory of Flow Machines.* (D. G. Randall, Trans.) Oxford: Pergamon Press
2. http://www.esru.strath.ac.uk/EandE/Web_sites/03-04/marine/res_resourcebkd.htm
3. http://www.marineturbines.com
4. http://www.esru.strath.ac.uk/EandE/Web_sites/03-04/marine/tech_concepts.htm#seasnail
5. http://www.mech.ed.ac.uk/research/wavepower/
6. http://www.lunarenergy.co.uk/
7. http://www.bluenergy.com/technology.html
8. http://www.alternative-energy-news.info/tidal-power/
9. http://www.daviddarling.info/encyclopedia/T/AE_tip_speed_ratio.html
10. http://www.windpower.org/en/tour/wres/betz.htm
11. http://www.reuk.co.uk/tidal.htm
12. http://tidalenergy.net.au/?D=50
13. http://www.hagglunds.com/
14. http://www.hagglunds.com/Upload/20060809110318A_en683.pdf
15. http://www.hagglunds.com/Upload/20060809110824A_en734.pdf
16. http://www.boschrexroth.com/mobile-hydraulics-catalog/Vornavigation/VorNavi.cfm?PageID=m3726&Language=EN
17. http://www.boschrexroth.com/borexmvz2/Detailview.jsp;jsessionid=FED4BF02414E01962DE5969FE68D40F8?publication=NET&ccat_id=30050&edition_id=58617&document_id=58605&view=zoom
18. http://www.wiebeck.de/filterbuch/rnormen.htm
19. http://www.automation.siemens.com/ld/ac-motor-high/html_00/asyn-kaefig/h-compact-plus/h-compact-plus.html
20. http://www.automation.siemens.com/ld/windkraft/html_00/windkraft.html
21. http://www.powergeneration.siemens.com/products-solutions-services/products-packages/wind-turbines/technology/
22. http://tattendorf.net/windkraft/techdetails.htm
23. http://www.spiegel.de/spiegelspecial/0,1518,474503,00.html
24. Baker, A. C. 1991, *Tidal power*, Peter Peregrinus Ltd., London

25. Lecomber, R. 1979, "The evaluation of tidal power projects", in *Tidal Power and Estuary Management*, eds. Severn, R. T., Dineley, D. L. & Hawker, L. E., Henry Ling Ltd., Dorchester, pp 31-39.
26. Hammons, T. J. 1993, "Tidal power", *Proceedings of the IEEE*, [Online], v81, n3, pp 419-433. Available from: IEEE/IEEE Xplore. [26 July 2004].
27. http://www.rmst.co.il/HVDC_Proven_Technology.pdf
28. http://www.abb.com/cawp/gad02181/c1256d71001e0037c125697b002a43b4.aspx
29. http://www.concreteinternational.com/pages/featured_article.asp?FromSearch=True&keywords=sea+water&srchtype=ALL&date=anytime&searchmonth=1&searchday=1&searchyear=2007&ID=2384http://www.manuli-hydraulics.com
30. http://www.teufelberger.com/
31. http://pages.unibas.ch/geo/mcr/Teaching/MeteoVorlesungen/Meteo4/Daten/PEDEEF/Pgs01_02.pdf
32. http://www.seaflex.co.uk/air_lift_bags.html
33. http://www.offshore-technology.com/
34. http://www.jwautomarine.co.uk/pr_lbs_pr.htm
35. http://www.fisheroffshore.com/
36. http://www.timberland.on.ca/catalogue.php?category_id=1175
37. http://www.seamarksystems.com/
38. http://www.hydramarine.no/winches/index.htm

C List of variables

a	Axial reduction factor
A	Area [m²]
A_h	Inner cross-sectional area of hose [m²]
A_I	Area of duct-inlet [m²]
A_m	Frontal surface of main pole [m²]
A_M	Mesh Area [m²]
$A_{m,c}$	Concerned frontal surface of main pole [m²]
A_O	Area of duct-outlet [m²]
$A_{P,I}$	Immersed platform area [m²]
$A_{P,P}$	Protruding platform area [m²]
A_t	Permeable area of mesh (anti – solidity)
$A_{T,w}$	Turbine working area [m²]
A_{TB}	Area of turbine base [m²]
C_D	Drag coefficient of turbine
$c_{D,m}$	Drag coefficient of main pole
$c_{D,P}$	Drag coefficient of platform
c_P	Overall power coefficient of the turbine
$c_{p,max}$	Maximum power coefficient of a wind turbine
c_{P1}	Power coefficient of downstream turbine
c_{P2}	Power coefficient of upstream turbine
d	Inner diameter of hose [m]
d_{2m}	Outer main pole diameter [m]
d_{AB}	Airbag diameter [m]
d_c	Diameter of buoy cable [m]
d_I	Inlet diameter of duct [m]
d_P	Immersion depth of platform [m]
F_1 & F_2	Reaction forces on each side of the turbine base [N]
F_B	Buoyant force [N]
F_D	Drag force [N]
$F_{D,C}$	Drag force at cut-in speed [N]
$F_{D,P}$	Total maximum drag force on platform [N]
$F_{D,P,I}$	Maximum drag force on platform (immersed part) [N]

$F_{D,P,P}$	Maximum drag force on platform (protruding part) [N]
$F_{D,R}$	Drag force at rated speed [N]
$F_{D,R,c}$	Corrected drag force at rated speed [N]
$F_{D,R,m}$	Drag force of main pole at rated speed [N]
F_{GB}	Weight force of generator base [N]
FoS	Factor of safety
F_R	Rope force [N]
$F_{R,C}$	Rope force at cut-in speed [N]
$F_{R,R}$	Rope force at rated speed [N]
$F_{R,R,GB}$	Rope force on generator base at rated speed [N]
$F_{R,R,sf}$	Rope force at rated speed including factor of safety [N]
F_{TB}	Weight force of turbine base [N]
g	Gravitational acceleration [m/s²]
h_{12} - h_{13}	Heights in U-manometer placed after the orifice plate [m]
h_2 - h_6	Heights in U-manometer placed before the orifice plate [m]
h_{20}	Height in U-manometer showing atmospheric pressure [m]
h_{ave}	Average height of h_2 - h_6 [m]
h_B	Height of buoy [m]
h_{GB}	Generator base height [m]
h_P	Platform height [m]
$h_{sl,m}$	medium sea level [m]
h_{TB}	Height of turbine base [m]
I	Amperage of generator [A]
I_m	Axial moment of inertia of main pole [m^4]
I_s	Axial moment of inertia of supporting pole [m^4]
K	Energy loss coefficient
K_L	Inlet loss coefficient of duct
K_M	Drag coefficient of mesh
K_{M1}	Drag coefficient of mesh first test series
K_{M2}	Drag coefficient of mesh second test series
L_{10aah}	Modified rating life of pump [h]
l_c	Length of buoy cable [m]
l_m	Length of main pole [m]
l_{m1}	Length of main pole between top end and junction [m]

l_{NT}	Water depth at neap tide [m]
l_P	Platform length [m]
$M_{B,B}$	Bending moment of main pole at base [Nm]
$M_{B,B,p}$	Resulting bending moment on each supporting pole [Nm]
$M_{B,J}$	Bending moment of main pole at junction [Nm]
m_c	Mass of buoy cable per meter [kg/m]
$m_{D,c}$	Displaced water mass [kg]
m_{GB}	mass of generator base [kg]
$m_{GB,sf}$	mass of generator base including safety factor [kg]
m_m	Mass of main pole [kg]
m_P	Platform mass [kg]
$m_{P,D}$	Mass displacement of platform [kg]
m_s	Mass of supporting pole [kg]
$m_{TB,c}$	Mass of buoy cable [kg]
$m_{TB,c,w}$	Mass of buoy cable in water [kg]
$m_{TB,sf}$	Mass of turbine base including safety factor [kg]
$m_{TB,total}$	Overall mass of turbine base [kg]
$m_{TB,total,R}$	Overall mass of turbine base in sea-water [kg]
n	Rotor revolutions per minute [rpm]
n_{1C}	Rotor revolutions of downstream turbine at cut-in speed [rpm]
n_{1R}	Rotor revolutions of downstream turbine at rated speed [rpm]
n_{2R}	Rotor revolutions of upstream turbine at rated speed [rpm]
n_G	Rated revolutionary speed of generator [rpm]
P	Overall rated power output of the turbine [kW]
p	Pressure [bar]
p_0	Atmospheric pressure [bar]
p_1	Pressure at the entrance of the test duct [bar]
P_{1C}	Cut-in power output of downstream turbine [kW]
p_{1C}	Pressure of downstream pump at cut-in speed [bar]
p_{1R}	Pressure of downstream pump at rated speed [bar]
P_{1R}	Rated power output of downstream turbine [kW]
p_2	Pressure at the exit of the test duct [bar]
P_{2R}	Rated power output of upstream turbine [kW]
P_C	Charge pressure of pump [bar]

P_{max}	Maximum power output of a turbine [kW]
P_x	Overall pressure on the left/right side of orifice plate [bar]
Q	Volume flow in duct [m³/s]
q_C	Flow rate at rated speed [l/min]
q_L	Volumetric losses [l/min]
q_R	Flow rate at rated speed [l/min]
$q_{total,C}$	Overall flow rate at cut-in speed [l/min]
$q_{total,R}$	Overall flow rate at rated speed [l/min]
R	Rotor radius [m]
R_1	Rotor radius of downstream turbine [m]
r_{1m}	Inner radius of main pole [m]
r_{1s}	Inner radius of supporting pole [m]
R_2	Rotor radius of upstream turbine [m]
r_{2m}	Outer radius of main pole [m]
r_{2s}	Outer radius of supporting pole [m]
r_B	Radius of buoy [m]
R_c	Gas constant [J/kgK]
Re	Reynolds-number
r_{GB}	Radius of generator base [m]
r_{TB}	Radius of turbine base [m]
s_m	Wall thickness of main pole [m]
s_s	Wall thickness of supporting pole [m]
T	Temperature [°C]
T_{1C}	Torque of downstream turbine at cut-in speed [Nm]
T_{1R}	Torque of downstream turbine at rated speed [Nm]
T_S	Specific torque of pump [Nm/bar]
u	Flow speed in hose [m/s]
U	Voltage of generator [V]
V	Flow velocity [m/s]
V_1	Flow velocity at the entrance of the test duct [m/s]
V_2	Flow velocity at the exit of the test duct [m/s]
V_∞	undisturbed wind speed in front of the rotor [m/s]
V_{AB}	Airbag volume [m³]
V_B	Buoy volume [m³]

V_C	Cut-in speed [m/s]
$V_{D,C}$	Displacement of hydraulic motor at cut-in speed [cm³]
$V_{D,R}$	Displacement of hydraulic motor at rated speed [cm³]
V_e	Wind speed after passing the rotor [m/s]
$V_{g\ max}$	Maximum displacement of hydraulic motor [cm³]
V_i	Displacement of pump [cm³/rev]
$v_{max,\ s}$	Max. Tidal current velocity on surface [m/s]
$v_{max,\ w}$	Max. Wind current velocity on surface [m/s]
V_P	Platform volume [m³]
V_R	Rated speed [m/s]
V_t	Flow velocity through test mesh [m/s]
V_{TB}	Volume of turbine base [m³]
$V_{TB,c}$	Volume of buoy cable [m³]
w_P	Platform width [m]
y	Height difference between Pitot-tube end and upper limit of fluid [m]
α	Horizontal deflection angle of turbine [°]
α_m	Angle of rope to vertical axis at medium sea level [°]
α_{NT}	Angle of rope to vertical axis at neap tide [°]
β	Grade of filtration
Δp_L	Pressure loss of pump [bar]
ΔV	Displacement shift of the hydraulic motor [cm³]
η_m	Mechanical efficiency of pump
η_W	Dynamic viscosity of water [kg/ms]
λ	Blade tip speed ratio
λ_1	Blade tip speed ratio of downstream turbine
λ_2	Blade tip speed ratio of upstream turbine
ν	Kinematic viscosity [m²/s]
ν_W	Kinematic viscosity of water [m²/s]
ρ	Density [kg/m³]
ρ_A	Air density [kg/m³]
ρ_C	Concrete density [kg/m³]
ρ_m	Density of medium [kg/m³]
ρ_W	Sea water density [kg/m³]
σ	Effective solidity

σ_B	Bending stress [N/mm²]
σ_{max}	Maximum allowable stress [N/mm²]
σ_Y	Yield stress [N/mm²]
Ω	Rotor angular velocity [s^{-1}]
Ω_{1C}	Angular velocity of downstream rotor at cut-in speed [s^{-1}]
Ω_{1R}	Angular velocity of downstream rotor at rated speed [s^{-1}]